PHASE I OPERATIONS

K500 CYCLOTRON OPERATING EXPERIENCE

P. Miller, D. Poe, J. Vincent

The statistics for the distribution of time use for the K500 cyclotron are given in Table 1.

Table 1--Time Distribution (1985)

Use Category	Hours	Percent of total
Research	2742	31 %
Development	301	3 %
Maintenance	866	10 %
Overhead	1170	13 %
Breakdown	2993	34 %
Off	689	8 %
Total	8760	

In Table 1 "Overhead" represents time used for tuning of the cyclotron and beamlines, ion source changes and deflector conditioning, i.e. operations other than research and development. The category labeled "Off" is time when no operation of the facility was scheduled, for example when no experiment could be scheduled or shifts during an extended shutdown which were not staffed. The category called "Breakdown" includes time when the facility operation was interrupted by equipment failures.

The beams provided by the cyclotron and the total time for each are listed in Table 2. The number of experiments completed in 1985 is 26.

Several modifications were made to the K500 rf system in 1985. These were described as proposed improvements in the 1983-84 MSU Annual Report.

Input Couplers

We had 5 input coupler insulator failures in 1985 which resulted in vacuum leaks and required replacement. The arc damage occurred on the air side of the insulator. During this time we obtained 3 planar alumina insulators which were brazed to concentric copper cylinders to adapt them to the coaxial coupler apparatus. These insulators did not arc on the air side; rather there was a tendency for metallization (copper) to be deposited on the vacuum side as if sputtered by a glow discharge (operating pressure was about 1.1 x 10 -5 torr with PIG ion source). Erosion of the braze joints between the insulator and the inner and outer conductors was especially severe. This problem was suppressed by adding ring electrodes.

Dee Stem Corona Rings

The corona rings were redesigned to provide positive clamping to the water cooled copper dee stem flanges. The joints contain 0.125" diameter plated coil spring rf gaskets. These springs also conduct heat dissipated in the rings by rf current.

The new corona rings were installed in November 1985 and January 1986. The temperatures during operation were satisfactory on 4 of the stems; the problem for the other two was traced to insufficient contact area caused by non-concentricity of the two flanges to which each corona ring is clamped. Since aligning those flanges was impractical the contact spring was removed from one joint to allow the ring to center itself on the other flange. The joint without the contact spring was then tack welded in 24 spots. The two rings assembled in this manner had the lowest operating temperatures.

As as a result of these modifications the operating temperatures are lower than before and we are able to increase the dee voltage to a level determined by conditioning of the dee gaps

(peak 89 kV during conditioning, 79 kV in operation).

Table 2-- Beams Provided by the K500 Cyclotron (1985)

Ion	E/A (MeV/u)	% Time	Hours
2 D 1+	25	1.2	40.9
4 He 1+	25	3.8	134.7
6 Li 1+	14	1.5	54.5
6 Li 2+	25	0.5	18.3
	35	7.8	277.6
7 Li 1+	10	1.6	55.7
7 Li 2+	25	1.9	66.0
	35	0.	3.5
12 C 2+	10	0.5	18.0
12 C 3+	15	1.6	56.8
12 C 4+	25	0.9	31.5
	35	4.8	169.5
14 N 2+	8	3.9	139.0
14 N 3+	15	4.4	155.1
14 N 4+	20	5.9	209.8
	25	0.5	18.6
	30	3.3	117.7
14 N 5+	35	14.7	878.5
	40	13.1	466.2
16 O 4+	25	0.2	5.5
16 O 5+	30	0.3	10.2
	35	2.9	104.5
16 O 6+	35	1.3	46.5
18 O 5+	30	1.3	44.5
20 Ne 4+	20	0.	3.5
20 Ne 5+	25	2.5	90.5
20 Ne 6+	30	0.5	18.1
22 Ne 5+	20	1.5	53.0
	24.6	7.1	253.6
22 Ne 6+	30	0.3	9.1
40 Ar 8+	20	0.	2.8
	Total:	100.0	3553.3

Dee Voltage Calibration

We constructed a filament source for control of the electron density during measurement of dee voltage using the bremsstrahlung endpoint method. A germanium X-ray detector was placed at a window in the cyclotron median plane to record the X-ray energy spectrum while rf power was applied to one dee at a time. The filament was installed in a PIG ion source modified for this purpose. It was inserted into the center hole in the lower pole of the cyclotron. The filament was heated with an alternating 20 kHz current.

This method has the following drawbacks:

- All three dees are not exposed to one window (shadowing of the X-ray source occurs).

- The magnetic field must be off during

measurements, as the electrons must move in the median plane (geometrical constraint on the X-ray path to the detector).

Other Projects

Other K500 cyclotron improvements were made in the following areas. The upper pole main vacuum gasket was cleaned and painted to prevent rusting. Water lines were installed in two of the valley liner sections. Thermocouples were attached to the electrostatic deflectors, liner and beam scraper to monitor their temperatures.

Projects are under way to address operation problems encountered this year. We expect to see better reliability of the K500 cyclotron when the improvements mentioned below are realized.

Several components in the rf final amplifier anode and screen grid power supplies failed and were replaced with better components. This is part of a larger project but we already notice better reliability.

The main magnet power supply current regulator and transistor bank failed after a power interruption. The protective Zener diodes have been replaced. Part of the planned upgrade to make this power protective circuit for the bank.

Valve orifices in the liquid helium transfer lines became blocked repeatedly with contaminants. This problem has been corrected operationally by adding filters to remove frozen particles from the liquid helium. More information about the status of the cryogenic systems is found elsewhere in the annual report.

Electrostatic deflectors do not hold as high a voltage in the cyclotron as they do in the deflector test stand. Improvements have been made in the insulators which support the cathode (see ref. 1). Other modifications for increasing the high voltage capability are being manufactured and tested off line. These include re-shaping the cathode cross section, testing different electrode materials and adding end covers to the deflector housing. A model of the K800 cyclotron hinged deflector is under construction and will be tested also.

ECR Ion Source

During this year the ECR ion source began operation and components for the injection beam line were built. some modifications of shielding walls and other K500 components were made in November and December 1985. The cyclotron was shut down on 23 Dec 1985 for installation of the beamline from the ECR ion source.

A new system which overcomes these deficiencies is being designed. It has 3 X-ray windows in the upper pole (one window per dee) with a filament for each one. A detector which can be pointed downward at the source of X-rays will be moved from one window to the next to record spectra from the different dees.

References

1. J.A. Nolen. L.H. Harwood, J.A. Kuchar, R.M. Ronningen, C.E. Scripter, J.E. Yurkon and A.F. Zeller. "Status of the Electrostatic Deflectors of the MSU K500 Cyclotron" Proc. 10th Int'l. Conf. on Cyclotrons and Their Applications, Apr. 1984, F. Marti, ed., IEEE, p. 571.

EXPERIMENTAL FACILITIES OPERATION

R.A. Blue, R. M. Ronningen, and N. Anantaraman

The major experimental facilities continued to be used routinely throughout the period of this report. A variety of experiments were conducted using the 60-inch scattering chamber, the S320 spectrograph, and the reaction product mass spectrometer. In addition three other target stations were employed for more specialized experimental set-ups. In this latter category the BM1 station was used to activate targets for off-line counting and to produce ^{13}N for tracer studies. The user's line served for in-beam gamma ray spectroscopy, for the neutral pion production experiments by the Stony Brook - Oak Ridge collaboration, for measurements of gamma-ray circular polarization, and for particle-gamma-ray coincidence measurements employing a 20-inch chamber. This chamber, which has a hemispheric lid, is now available for general use. The third area now being utilized for more varied experiments is the neutron chamber, station. The chamber developed for neutron investigations including coincidences between neutrons and charged particles, continues to be employed for that purpose, but with that chamber removed the station serves for other experiments such as the detection of high-energy gamma rays. Thus, within the limitations of space, the laboratory has been able to accomodate a diversity of experimental equipment.

During this period the beam transport system has not undergone any basic changes in design though there have been some improvements to increase operating reliability. In particular the multi-output DC supply that powers several magnetic beam transport elements had long been prone to failures of the germanium output transistors which had become expensive and difficult to obtain since they are obsolete. A redesign of the transistor banks has permitted the substitution of modern silicon transistors which provide much higher operating reliability. The replacements have been installed whenever an output failed with the result that all of the more failure-prone channels have been replaced. To date there have been no failures in the new transistor banks.

The control circuits for this power supply were partially reworked to make them compatible with the new control system. The operator interface now makes use of a color CRT with software-assigned knobs. As an initial proving ground for the control system design, this station has been equipped with a succession of two varieties of touch screen, a track ball, and currently a mouse as the operator's interactive input device. An upgrade of the controls to the new system design has also been undertaken for the 60-inch chamber. In this case the original stepping motor drives and remote position readouts came to the end of their useful operating life. The motors and the encoders from the original installation are still in good working order and will be used in the reworked control system.

Vacuum system operations for the beamlines and experimental chambers have continued with no significant new developments. Ion pumps which have been in continuous operation for about three years are generally reaching the point where they require the replacement of the titanium grids while those pumps operating under abnormally high gas loads have already been serviced two or three times. The service requirements for cryopumps are also somewhat variable, but a year of normal operation is perhaps a typical interval for cold head service beyond the routine cleaning of contaminated

pumping arrays and helium gas recharges. We have elected to do cold head repairs inhouse rather than to rely on factory exchange servicing. One problem which continues to limit the general applicability of the closed-cycle cryopumps is their sensitivity to hydrocarbons. For example isobutane, used as a counter gas in thin-windowed counters, quickly leads to deteriorating pump performance when it is condensed into the pumping array. As a result experiments using gas counters in the 60-inch chamber have come increasingly to rely on a turbomolecular pump in preference to a cryopump. Fortunately we recently acquired as used equipment four large turbo pumps, one of which is to be permanently installed on the chamber.

COMPUTER ADDITIONS AND UPGRADES

R. Fox, R. Au, L. Foth, B. Pollack, and A. VanderMolen

Introduction

This contribution will discuss upgrades and additions to the computer systems at NSCL completed in the last year. These are functionally divided into three categories: Control system, Data acquisition system, and General Computing. The control system category includes hardware and software support and additions to both the K800 and K500 control systems. The data acquisition system includes support of both front end acquisition systems, and back end VAX based analysis and support software. General computing will be a category which we will use to group all progress which does not fit well into any of the categories above.

Control system

The control system has seen additions and upgrades to both the K500 and the K800 control system. While much of the progress has been devoted to bringing the ECR on line, some progress has been made in other areas.

This last year has seen the successful addition of the ECR to NSCL's arsenal of accelerator support equipment. In addition to the non-trivial hardware construction challenges, the ECR has also presented us with a unique set of control requirements. These have been met at the hardware end with the VME based control system discussed last year[1] supplemented by commercially available interface devices where time did not permit the development of the serial device controllers featured in that system. The user level control consists of a touch screen grid allowing simultaneous monitoring of all pertinent ECR variables. Soft assignable knobs also allow control of up to four variables which may be either single devices or "ganged" pseudo parameters. Assignment of control knobs to devices is easily performed by touching regions of the screen which are armed as "soft buttons". Data logging and parameter plotting have also been implemented. Recently an additional console was installed to permit control of the ECR and associated injection controls to the K500. This console was installed in close physical proximity to the present K500 console.

A failure of an earlier 8080 based control system which controlled the K500 beam line, gave us an opportunity to test the adaptability of the K800 control system to unusual device interfaces. In less than a week, the 8080 based system was replaced with one of the VME 68010 local stations, and control of the beam line was restored. The addition of a touch screen and knob set to the beam line control console allows control over the beam line in a manner similar to that of the ECR.

The K500 control system continues to run, although the beam line control replacement also eventually picked up several control elements from this 11/34 based system. Upgrades to the K500 have been supported. The installation of phase slits and an upgrade to the K500 viewer probe involved alterations of 11/34 software and new interfacing hardware.

We hope that next year the K800 control will replace additional segments of the 11/34 system. We hope to accomplish this initially by the construction of a VME<->UNIBUS interface which will allow the 68010's access to the multi-port memory used to store control state information. This will allow the console functions of the K500 system to be moved to K800

console systems which will be ready in this coming year. Eventually, the 11/34 control functions will also be taken over piecemeal by 68010 local stations. Additionally, next year should see the addition of several more elements of the K800 to the control system.

Data acquisition system

This year has been mostly a consolidation year for the data acquisition system. We have offered continuing support and service from the dual 68010 fast acquisition front end reported on last year[2], while continuing to allow access to the slower LSI-11/23 based system. Additionally work has proceeded in two major directions.

Our experiences with the 68010 based acquisition system have led us to revise the design of this system and to implement instead a pipelined mode of operation. A single 68010 continually acquires data into memory shared with a second 68010. This data is formatted and shipped back to the VAX-750 by this second 68010 by means of a DEC DR-11W interface. The second processor also performs run control operations. We have also revised the design of the VME<->CAMAC interface to support experiments which require up to eight acquisition CAMAC crates. The first experiment using this system is being set up at the time of writing. In the next year we will complete a second system of this type to allow continual service to the two data acquisition U's currently operational.

As the experimental and front end system complexity grows, we believe that it will be important to have tools which allow the experimenter to set up at least the basics of an experiment without knowing the details of either the front end or the CAMAC devices used. Work on an experiment editor has been underway in the last year, and a prototype system which should allow simple experiments to be set up in purely "physics terms" has been completed. The system maintains a data base of CAMAC modules, and the FNA's required to set up, acquire data from and reset them. The experimenter uses a screen based special purpose CAMAC crate editor to "stuff" CAMAC crates with devices needed for the run. Moving the cursor around on the screen, the user names inputs on each module, and later simply specifies which inputs are to be read for each bit set in the pattern register. Scaler readout, and live time scaler displays are generated in a similar manner. The program generation system generates front end independent experiment description files which are then automatically translated into front end specific code. The particular front end system is then assembled and an experiment start up command file is written.

Given the experience gained by test runs of the streamer chamber CCD camera acquisition system[3] additional hardware was constructed to allow the 68010's some variation in the time required to acquire each pixel. This time variation arises as a result of the set up time required for the 68010 CPU's to enter their high speed loop mode on the first pass through each pixel acquiring loop. We have added FIFO buffers which allow the 68010's to miss a pixel arrival time when doing this setup and "catch up" during the remainder of the loop.

Finally, physical memory on the two data acquisition VAX 750's was expanded to 5 megabytes. This has allowed on line analysis programs to run with fewer page faults, and hence analyze a larger fraction of the incoming data on line.

General purpose computing

For the purposes of this report, general purpose computing has been rather arbitrarily classified as computing which does not fall under the headings already discussed. This includes additions to the laboratory Administrative Data Processing (ADP) system,

word processing support, graphics support, hardware and software upgrades and additions to the laboratory's VAX-7xx computers, and additions and upgrades to the laboratory CAD system.

In the last year, several pieces of software have been acquired both from commercial vendors and from the public domain. In addition, some in-house support effort has been directed towards the enhancement of software already owned. For ADP, we have purchased the DEC Datatrieve file management/database system as a migration path upwards from the rather limited capabilities of the current ADE based system. ADE is capable of writing its table files in Datatrieve readable format, so one to one migration should be relatively simple. We have constructed two full scientific font sets for the LN01 laser printer for use with the MUSE/WORDMARC word processing system. These fonts allow high speed draft copy to be produced at either 10 or 12 pitch.

We have acquired the National Center for Atmospheric Research (NCAR) graphics systems as well as the University of Wisconsin's TopDrawer systems for the production of presentation and publication graphics. We have purchased an HP7475A color plotter to allow hardcopy output from these presentation graphics systems. Lower quality black white graphics output is of course still available via the Trilog matrix printer.

Last year saw the purchase of an INTERGRAPH CAD/CAM system. While this system was used primarily for mechanical drawing, its use has expanded to electronic circuit board design and layout. We have expanded the number of graphics entry stations from the original two to a total of six, and the number of hardcopy plotters from one to two to meet the increased demand for this resource.

Last year it was observed that a lack of physical memory on the VAX-780 forced this machine to run in a heavily disk I/O bound mode due to a high page fault rate. This fact taken together with the increase in physical memory requirements of VMS 4.x versus VMS 3.x forced us to delay the installation of VMS 4.1 on the VAX-780 and the ANALYSIS VAX-750 which runs the 780 disks when the 780 is not in service. This year we have doubled the 780 physical memory from four to eight megabytes. The resulting increase in performance has allowed us to upgrade the operating system to VMS 4.2 on all lab computers. Physical memory was also added to the ANALYSIS VAX 750 bringing it up to a full complement of 8 megabytes of physical memory.

Hardware upgrades to the TEST machine include the addition of physical memory (also bringing it's memory to 8 megabytes), and the addition of an AED color graphics display terminal. With these additions, the TEST machine completes its transition to a full fledged secondary analysis processor.

Conclusions

This last year has been a busy year for the computer group at NSCL. Extensive progress has been made in the K800, control system, the data acquisition system, and meeting the general purpose computing needs of the lab.

In the forthcoming year we can look forward to an increase in the number and complexity of devices controlled by the K800 controls system. We can also look forward to the implementation of general control consoles for the K800. As experiments grow in size and complexity, we anticipate the need for faster front ends, and perhaps front ends which are more loosely coupled to each other and the VAXes to which they feed data. We can also look forward to the usual increase in demand for general purpose computing facilities.

References

1. "Phase 2 Control system I: Overview" R. Au et al. 1984-1985 Annual Report Cyclotron Laboratory Michigan State University
2. "Fast Data Acquisition System" A. VanderMolen et al. 1984-1985 Annual Report Cyclotron Laboratory Michigan State University
3. "Development of CCD Cameras for Streamer Chamber" S. Angius et al. 1984-1985 Annual Report Cyclotron Laboratory Michigan State University

NUCLEAR ELECTRONICS DEVELOPMENT

M.R. Maier, M. Robertson

The planned experiments at NSCL pose a challenge to the electronics development, since they may either start with a few detectors, expanding to larger numbers (for example, a multi-detector hodoscope), or they may start out big (for example, the planned 4π detector discussed elsewhere in this Annual Report).

Both approaches have different solutions: With the experiments that start out small, we have packed as many electronic processing channels (discriminators, coincidences, etc.) into one NIM module as possible. Lack of front panel space then occurs -- there is not much room for controls and connectors. This usually limits the number of channels placed into one module (the board space inside the module is hardly ever a limitation). An extreme case of cramming functions into one module is the octal constant fraction discriminator.

We intend to pursue this solution by building a quadruple shaping amplifier in a single width NIM module.

However with the increasing number of detector-processing electronic channels, the difficulty of adjusting gains and thresholds increases dramatically, and the number of cables begins to dominate the experiments.
Therefore, we are pursuing a different design of detector-processing electronics. We intend to extensively use computer control, via CAMAC for example. Fortunately, there are commercial modules available, which were designed initially for high-energy physics experiments. For 4π detector experiments in particular, we plan to use the FERA ADC system and the associated connecting bus system ECL line as introduced by LeCroy. This has the following advantages:

a) All modules will be controllable via CAMAC, which dramatically simplifies the preparation of an experiment. The parameters can be set and read from the computer, which makes control very easy and transparent.

b) The ECL line uses very inexpensive multi-line cables, which reduces the cable labyrinth associated with the old-style experiments.

c) The FERA system allows fast and selective readout of valid information. This permits trigger schemes which rely on digitized ADC information, which also can be controlled and changed from a computer. These features allow experiments of complexity approaching high-energy physics.

We can't use the results of high-energy physics experiments because they are not precise enough; similarly, commercial modules made for high-energy physics experiments are too crude to offer the degree of precision we need. For instance, there is no modern commercial peak-sensing ADC in CAMAC that allows spectroscopy with semiconductor devices. Commercial units rarely have the rate capabilities and resolution needed in nuclear physics experiments.

However, there are many techniques to achieve these goals with the old 'NIM style' processing electronics. We intend to incorporate these techniques as we develop modules for future experiments at NSCL.

Present Status

Modern multiparameter experiments tend to adopt the high-energy physics architecture; many detectors are used with relatively simple electronics and many ADCs and TDCs. Instruments required for these experiments are a preamplifier, a main amplifier or shaper, a discriminator, and an analog-to-digital converter (ADC) for every detector.

In these experiments, an 'event' occurs when a pattern of detectors gather useful

information (hits). Patterns must be identified as fast as possible so analog energy pulses won't be delayed too much. Therefore, fast discriminators and fast logic operations (e.g. Boolean AND) are needed to minimize the number of cables, which delay analog signals. Minimizing the delay of propagation through these units is more important than maximizing the rate capability. In order to serve our needs, we have built special electronic modules that either are not commercially available or are more expensive to buy than to build.

At present, we have finished 20 4X4 four-fold, four-input logic boxes. One channel of these units generates the Boolean AND function from four inputs. The propagation delay is less than 5 ns from input to AND output, less than 10 ns to the one-shot output, and less than 15 ns to the slow NIM output. Commercial coincidence units usually have longer propagation delays.

We have started to build 20 quadruple gate generators for the digital signals. These units accept fast NIM signals, and generate delayed fast and slow NIM signals, where delay and width can be varied between 10 ns and 100 μs. The units also include the 'blinker.'

An interface was built between the CCD cameras for the streamer chambers experiment and 68000 data acquisition. This is used to study electronic storage of streamer chamber pictures. First experiments using this device at LBL were successful.

Future Developments

We will build or develop the following modules:

1. Quad fast amplifiers, 3 outputs, -2.5V out.
2. Quad slow shapers; fast and slow outputs, slow output shaping times 1,3,5,7 μs to 10V uni- and bi-polar. Fast out: integration and differentiation 10ns to 300ns, to -5V.
3. Octal CAMAC constant fraction discriminator; eight independent thresholds, with dead time and output pulse width control via 8-bit DACS. Output: ECL line, one for dead time, one for separate width.

We intend to concentrate further development work on special electronics, making use of 'old' techniques from nuclear physics. These become attractive as the complexity of the experiments grows, and as better electronic devices become available.

One item that we will pursue in the near future is the use of pulse shape discriminators to identify particles in inorganic scintillators. This will help the construction of very compact multidetector arrays for light particles and gamma rays.

Clearly, an important feature of the electronics developent program is the close collaboration between the electronic design group and nuclear scientists, leading to an appropriate and rapid response to the needs of particular experiments.

HELIUM LIQUEFIERS, THEIR OPERATION, AND ASSOCIATED EQUIPMENT MODIFICATIONS.

H. Laumer, A. Gavalya, J.A. Nolen, M.L. Mallory, J. Yunker, R. Zarobinski

The successful operation of liquid helium cooled superconducting magnets, as required by the program, was sustained in spite of a number of vexing problems. The major problem was plug formation in the cryogenic lines leading to interruption of liquid helium flow and in another case to the rupture of a liquid nitrogen precooler heatexchanger of the CTI-1400 refrigerator. These problems are reported more extensively in other sections of this annual report. The liquid helium required for the operation of the K-500 and K-800 cyclotron magnets in the past year was supplied by essentially the same equipment as reported in previous annual reports. The CTI-1400 compressors (total capacity 14 g/s of helium) have been phased out. A third screw compressor, which increases the total compressor capacity from 50 g/s to 80 g/s, was brought on line. While maintenance requirements of the screw compressors are moderate, a few problems were encountered in the past year. Two staged compressors are used to supply 50 g/s. The high pressure stage developed an oil leak in its compressor housing; the manufacturer recommended an exchange and this was done.

As noted in the 1984 annual report, it was found that oil was carried by the helium stream to the cold box. Modifications to the oil removal hardware were completed and as a result performance improved. An aerosol monitor[1] was acquired and presently measures oil contamination levels below 30ppb. Due to the heavy contamination of the helium liquefiers by oil carryover before the hardware changes, we decided to clean the high pressure piping of both liquefiers by flowing solvent through them. The CTI-1400 was cleaned first as a test for the procedure. Freon-TF was circulated with a pump. A total of about 15 gallons were circulated in three sequential operations each diluting the remaining oil. Freon was also flowed through the charcoal adsorbers in this procedure. To clear the solvent from the piping it was purged with nitrogen gas. A vacuum roughing pump operated for 72 hrs. then removed the remainder of the solvent. Startup of the refrigerator proceeded normally. Plugging of the liquefier was noticeably reduced and the production capacity also improved (20%).

After the success of this clean up, we performed a similar operation on the Blue (CCI Liquefier -421) refrigerator. We elected to flow methylene chloride through this unit. Its vapor pressure is somewhat higher than that of TF, promising faster removal. The cost of solvent also favors methylene chloride; though, its greater toxicity requires more care in carrying out associated tasks. The solvent was circulated with a gear pump capable of maintaining a pressure of 60 psig (pounds per square inch gauge). The flow rate of the solvent through the piping was in the range of 15 to 25 gallons per hour. The contents of three 55 gallon drums were recirculated through the high pressure piping of the heatexchangers as well as through the charcoal adsorber beds (5cuft) for 30 hours. The cleanup was concluded with a once through flow of two barrels of new solvent. Following this, the time consuming task of getting the methylene chloride out of the piping and charcoal adsorbers commenced. A regimen of flowing nitrogen gas, heated to 86° C, through one adsorber bed while vacuum pumping the other with a liquid nitrogen trapped roughing pump, was started, with the procedure alternating adsorber beds every few days. The roughing pump trap assisted in gauging progress. The rate of trapping methylene cloride was initially 6 liters per day and tapered off at

the end to 20 ml per day. The total solvent removal time was a month. It can, we estimate, be shortened to 2 weeks if higher temperature purge gas flow is initiated from the start. Also the procedure would have taken much less time, if the charcoal beds had not been included. Since the completion of the cleanup, the liquefier has now operated for five months without the necessity of a coldbox warmup.

The expansion engines associated with the Blue Refrigerator have all been modified to use new push rod seals and seal housings. Also a new piston rod housing incorporating a simpler linear bearing and polyurethane seal in conjunction with baffles installed to reduce convection currents of cold helium gas have resulted in quite reliable operation. The two most frequently operated engines have logged over 3000 hours since the last major maintenance period.

The performance of the refrigerator was last measured in December 1985. The oil cleanup had been completed and the new compressor raised available gas flow to 80 g/s. The refrigerator performance was measured to be 420±15 watt (heater immersed in receiving dewar) and simultaneously the dewar liquid level rate of rise was 138 l/hr. The refrigerator specifications call for 400 watt and 100 l/hr rate of rise. Under the operating conditions to achieve this performance level, the low pressure side heatexchanger pressure drop is found to be high. This could lead to magnet coil cryostat pressures that are too high for safe magnet operation. The refrigerator design called for 3 psig at the point where cold gas is returned from cryogenic devices; instead pressures near 12 to 13 psig are observed. This will have to be corrected when the full refrigerator performance is needed to operate all the devices requiring liquid helium planned for the future.

Impurities in the supply helium gas can be a serious problem for operating liquefiers and liquid helium distribution equipment. Over the years diagnostic equipment has been acquired as it became obvious what is needed. We presently monitor for water vapor with a hygrometer.[2] The water vapor concentration has varied from 20 ppm to 0.3 ppm. The high value usually is encountered at startup of the refrigerator after maintenance operations, while the low concentration is attained after a few weeks of continuous operation. Oil contamination at the 100 ppm to 1 ppm level is measured with an oil check kit;[3] this is useful for monitoring intermediate stages of the oil coalescers. Below the 1 ppm level an aerosol monitor is used. This is useful in monitoring oil concentration entering the refrigerator coldbox. To monitor other sources of contaminants, such as N_2, H_2, and Ne, we have put in operation a system similar to that built by R.J. Walker.[4] We acquired a monochrometer[5] which, in conjunction with a glow discharge arc cell, during initial trials, appears to be capable of sensitivities of 0.1 ppm for N_2, 0.3 ppm for H_2, and 0.2 ppm for Ne. Looking back on our experiences we strongly recommend these or similar monitoring devices. However most are not easy to use since drifts in calibration occur for many reasons so that absolute concentration measurements are not routine. If monitoring equipment is used from initial operation of a liquid helium refrigeration system, potentially many operating hours can be saved.

References

1. Aerosol Monitor Model P-20 made by ppm, INC., Knoxville,Ten.
2. Model System I Hygrometer, from Panametrics.
3. OilCheck(TM)Kit made by Balston, Inc.;Bulletin TI-200B.
4. Detector for Trace amounts of Nitrogen in Helium, R.J. Walker, Cryogenics 26, 297(1986).
5. Model 270, 0.35 Meter Scanning Monochrometer, McPherson Division of S.I. Corporation.

1400 LHe REFRIGERATOR LN HEAT-EXCHANGER RUPTURE

M.L. Mallory, H. Laumer, J.A. Nolen, J. Yunker, R. Zarobinski, and R. Powers[a]

On December 16, 1985 at 8:10 AM, a loud bang was heard coming from the 1400 LHe refrigerator cold box. Subsequent investigation verified that the LN-He gas heat exchanger had ruptured from the liquid nitrogen circuit to the vacuum space of the cold box. The following sections describe the various results obtained in our efforts to understand this failure. Although no definitive explanation for this rupture can be stated at this time, a series of improvements were implemented and they are listed.

Investigation Discoveries

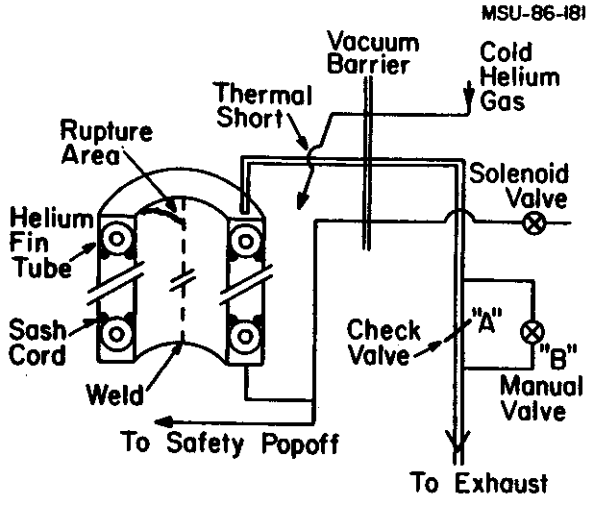

Fig. 1 A schematic drawing showing the various connections to the LN heat exchanger of the 1400 LHe refrigerator.

Figure 1 is a circuit diagram of the liquid nitrogen-helium heat exchanger. The nitrogen circuit is the shell of the heat exchanger and has two ports. The top port is the boiloff gas exit from the heat exchanger. It exits through the cold box vacuum jacket. The line then goes to a check valve (A) and a parallel bypass valve (B). This line exhausts to the ambient air. The bypass valve is normally opened only to cool down the refrigerator cold box. A cool-down occurred approximately two weeks before the rupture. After the rupture it was found that the valve had inadvertently been left open during this period. In the past, this has happened and this line became plugged presumably due to frost from water vapor in the air. It is surmised that this could have happened here. Also after disassembly of the cold box a near contact (thermal short) of the low temperature helium return gas (≈ 5°K) and the nitrogen exhaust line was discovered. The possibility exists that this near contact point could cause a freeze out point of condensible gases in the exhaust line. After repair and reassembly of the 1400, no improvements in the refrigeration capability were detected, indicating that very little energy was involved in this near contact point. Secondly we have previously operated continuously for up to 6 months or longer with this near contact and have not had an exhaust line plugging problem.

Even with blockage of the exit line, the heat exchanger should be protected. The supply port is shown in Figure 1 and enlarged in Figure 2. The supply port is connected to a safety popoff. The line also connects to an automatic refill solenoid valve. The safety popoff was checked after the rupture and found to be set at 48 psi gauge (or the pressure on the heat exchanger shell would be 63 psi relative to the cold box vacuum). The refill inlet line is connected to the liquid nitrogen storage tanks. The storage tanks (2 - 3600 gallon dewars) normally operate at 35 psi. However the storage tanks ran out of LN approximately 12 hours

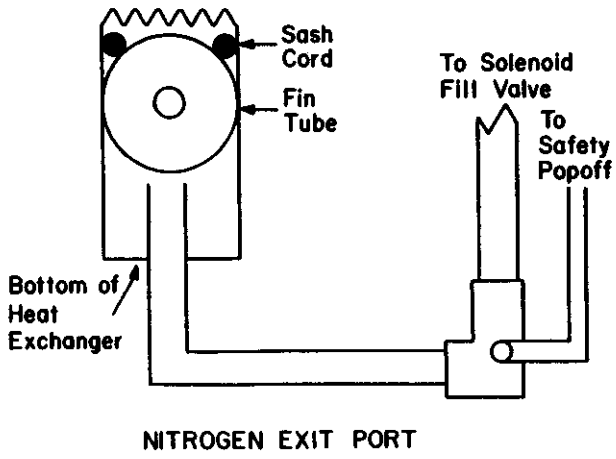

Fig. 2 A drawing showing the inlet connection of the LN heat exchanger. A section of piping is common to both the fill line and safety popoff and could become blocked at the low point, thereby causing a common mode failure of these lines.

before the accident and the tank pressure dropped. This loss of LN had not occurred in about 5 years of dewar operation. With the pressure on the LN supply system at 0 psi it became possible for the nitrogen boiloff gas to leak out the inlet valve line. An experimental measurement of the inlet control valve leakage rate was made and a leak rate of N_2 gas at room temperature of 29 atm cc/sec at 48 psi differential pressure was obtained.

The heat exchanger shell consists of two concentric stainless steel tubes. The ruptured inner tube is .062" thick x 6.8"ID x 30" long. It is supported by welds at each end. The rupture initiated at one of these welds. It did not collapse from an instability condition, but tore from the weld. The theoretical stability limit of the inner tube of the heat exchanger is 117 psia if supported adequately by the welds at each end. The stability limit of an unsupported tube is 42 psia. The maximum recommended working pressure (ASTM code) for the supported tube is 42 psia.

Possible Scenarios

Two scenarios were investigated in depth. Both assumes that the exit line was blocked. The first scenario assumes the following. First, the LN fill valve opened and filled the shell with LN as normal. Then the inlet valve closed but leaked at the measured rate. With this condition, the exit blocked by atmospheric moisture and the inlet valve closed but leaking, it is easy to show that a room temperature helium gas input rate of $\leq$ 0.1 gls would generate enough heat in the nitrogen shell to cause its pressure to rise to 60 psia. It is conceivable that at such a pressure the inner tube collapsed by tearing at a thin spot in one of the end welds. This pressure is above that for the unsupported tube, but below that for a supported tube.

In order for the pressure to rise higher than 60 psia, the second scenario assumed the popoff line had become blocked. There is a common section of piping connecting the popoff and inlet valve that is the lowest point of the system. One possible blockage proposed was that this inlet line was exposed to cold argon gas which then solidified in the lowest point of the line and blocked it. A gradual boiloff then allowed the pressure to buildup and exceed the exchanger rupture point. It was speculated that cold argon gas could have come from the LN storage tank which had not been warmed up in 5 years of operation. To check this possibility an experiment to detect argon from one of the LN dewar after it was warmed up was performed. No argon was detected. Also the level sensor line for the LN dewar is at the very bottom and it probably would have become blocked if there were an accumulation of "trash" in the bottom of the dewar. No blockage has ever been detected on the level sensor lines.

Modifications Implemented

The inner shell of the heat exchanger was repaired and reinforced with thick stainless steel rings. The heat exchanger was then hydrostatically tested to 100 psi. A pressure maximum indicating gauge was added to the popoff line. A large check valve that can easily take the full nitrogen boiloff in any situation was added to the nitrogen gas exhaust line eliminating the need for a manual bypass valve. It is also recommended that any new refrigerator nitrogen heat exchanger should have its popoff line independent of the fill line, and not be connected to the lowest point of the heat exchanger.

---

a. Powers Associates, Inc.

MICRON SIZE FILTERS IN LIQUID HELIUM TRANSFER LINES

M.L. Mallory, H. Laumer, A. Gavalya, J. Yunker, R. Zarobinski, J.A. Nolen

Introduction

After a planned upgrade of the K500 cyclotron, during July 1985, the startup of the accelerator in August was characterized by an increased rate of occurrence of cryogenic problems. Figure 1 illustrates this, where each tick mark as a function of time shows an accelerator cryogenic problem resulting in a delay of K500 operation. A major effort at understanding this problem was undertaken. A solution has been found that makes a significant improvement in cryogenic reliability. This solution is the addition of a 2μm stainless steel filter in the liquid helium stream. Presently it is not evident what initiated the cryogenic problem or what may have enhanced an existing one. Efforts are continuing to clarify this question. In the following sections, the information obtained concerning this cryogenic reliability problem are described.

Liquid Helium Supply Interruptions

Figure 2 is a schematic drawing of the cryogenic distribution system to the K500 cyclotron. The refrigerators make liquid helium which is stored in a dewar. The storage dewar is pressurized and continuously transfers liquid helium to the K500 cyclotron. In the distribution line are located various control valves that allow metering of the liquid helium to the K500 coil cryostat and to the vacuum cryopanels.

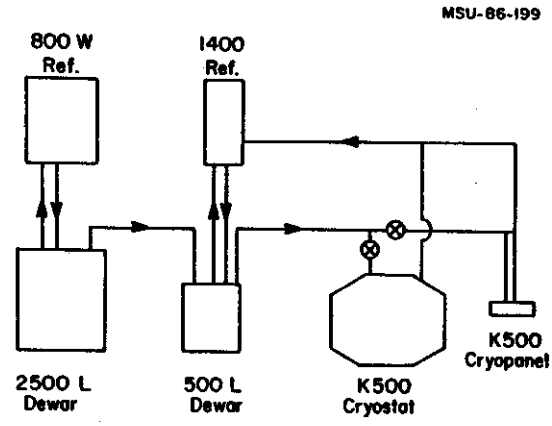

Fig. 2 A schematic drawing of the liquid helium distribution to the K500 cyclotron. The plugging was first located in the valve going to the K500 cryostat.

The first indication of a cryogenic distribution problem was a decline in liquid

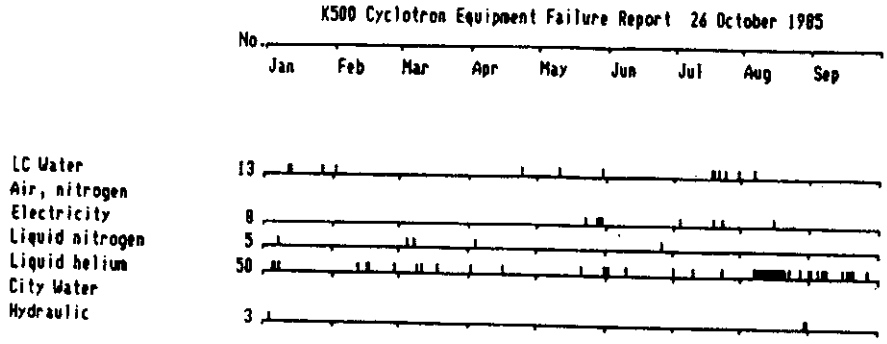

Fig. 1 The equipment failure report of the K500 cyclotron showing the increase in incidents due to problems with the liquid helium distribution system.

helium level of the K500 cryostat. This decline in level was diagnosed to be due to a plug in the cryogenic distribution system. The normal procedure to open a plugged line is to stop the helium distribution, warm up and purge the transfer line. This requires considerable time. After experiencing several of these line plugging episodes, pressure tap points were added along the distribution line and were continuously monitored. The information from the pressure sensors concurred with the line plugging assumption and tended to indicate that one section of the distribution system was the major plugging point. Also in this operational period it was found that the plug could be removed by the simple procedure of just stopping the transfer for one to five minutes. This procedure was christened as "burping" the transfer line. In figure 3 is shown the pressure drop across a section of transfer line as a function of time. A sample of burping the line is also shown. This burping procedure allowed cyclotron operations to be interrupted for a shorter time period (<1 hour). However the intervals between burping the line varied from 3 to 8 hours still resulting in a considerable down time problem.

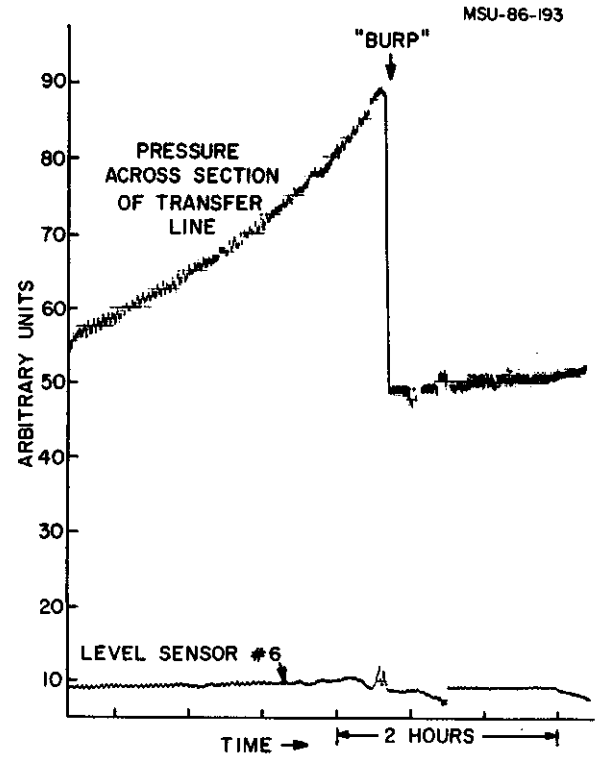

Fig. 3 The pressure across the helium transfer line versus time is shown. The dewar pressure in about 10 psig and the cryostat is ~6 psig. A short closing of the cryostat valve (burp) would restore the transmission of the liquid helium to the cryostat. The liquid helium level in the cryostat is also shown and reflects pressure changes in its level.

In an effort to locate the precise plugging point, the valve seat in the control valve f the K500 cryostat transfer line was removed. This stopped the plugging problem in this section of the line, but it then appeared at another location. This result suggested a model of something flowing through the distribution lines that could coalesce at critical locations, for instance at places where the velocity of the fluid changed. The coalesced particles would break loose and plug a small aperture. In an effort to detect such a plug, the K500 cryostat valve seat was reinstalled and upon plugging was rapidly removed (matter of minutes) and examined. All efforts at trying to detect a "solid" blockage failed.

This model also led to the installation of a 200 mesh (~.004" spacing) screen on the entrance of the transfer line located in the storage dewar. This screen filter did not alter the line plugging problem.

Helium Refrigerator Operating Mode Experiments

An effort to correlate the plugging with changes in operating modes of the refrigerator system during the July shutdown was attempted but no satisfactory explanation was found. The K500 supply dewar receives liquid helium from the CTI 1400 refrigerator and/or the 800 watt refrigerator and some changes were made in these lines during July. An experiment to supply the K500 dewar only from the 1400 refrigerator resulted in a 13 day period of no line plugging.

Before this could be investigated further, the 1400 refrigerator had a heat exchanger failure, necessitating complete dependence on the 800 watt refrigerator, but this strongly suggested a difference in the refrigerators.

An experiment based on the assumption that the helium gas supply had been contaminated was performed. The entire helium gas inventory was replaced. No change in plugging rate was observed.

Spectrographic measurements of the helium gas were performed and nitrogen at the 100 ppm was found to be the major gas impurity. An operational program of recycling the 80 K traps reduced the nitrogen impurities to the 1 ppm level in the ambient gas, but did not stop the plugging.

Filter Experiments

A transfer line section containing a 2 micron filter with a low C_v was built. It seemed to solve the plugging problem but the pressure drop across the filter resulted in problems of maintaining adequate liquid supply to the cyclotron, without making large changes in the dewar pressure. Raising the pressure also creates flashing problems in the K500 cryostat.

Next a 2 micron filter with a large C_v was located and it is shown in figure 4. This filter could be inserted into the bayonet end of the transfer line connecting the 800 watt refrigerator dewar to the K500 storage dewar and resulted in successful line operation.

A filter box shown schematically in figure 5 has now been built. It has dual filters and isolation valves. A sample line that connects to an optical spectrometer is provided. This filter box has been installed in the transfer line to the K800 magnet. The K800 line has also shown evidence of plugging. The first attempts at analyzing material trapped in the filter box has indicated an increase in neon and hydrogen

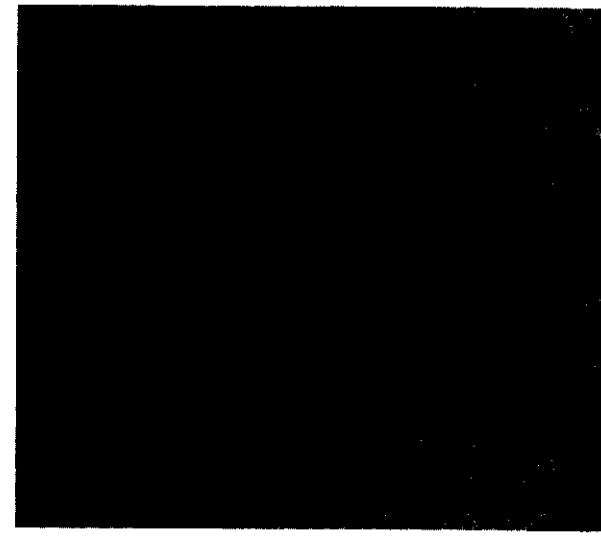

Fig. 4 A photograph of the 2 micron stainless steel filters is shown. It is 18" long and 1/2" in diameter. The liquid helium pressure drop across it is undetected.

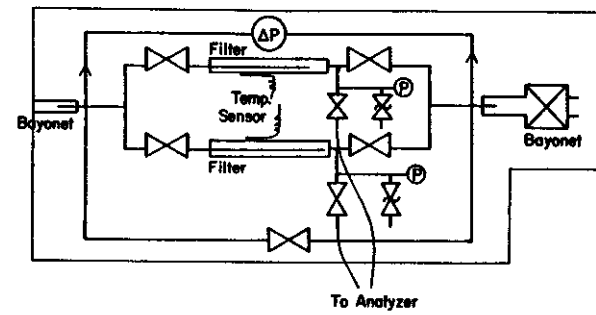

Fig. 5 A schematic drawing of the filter box build to measure what is being trapped in the filters is shown.

content versus samples of the ambient helium gas (Fig 6).

Difference in the 800 Watt and 1400 Refrigerator

The successful operation of the line with the 1400 refrigerator has resulted in the comparison of differences in the helium refrigerators and two are noted below. The 1400 has two small filters located in the cooldown stream at very low temperatures. It is assumed that these filters could trap out gasses such as

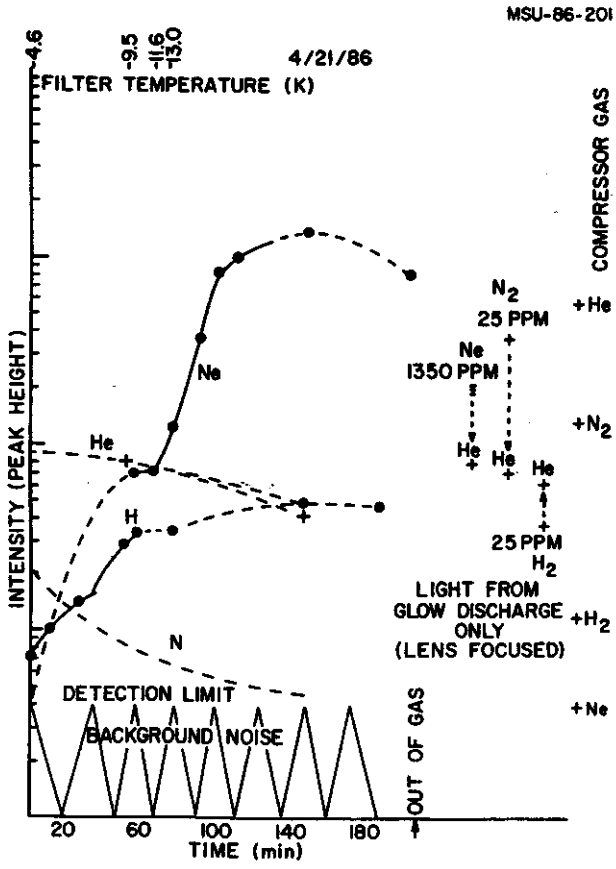

Fig. 6 The relative intensity of the spectrometer lines for material trapped in the 2 mm filter is shown as a function of time after isolating the filters. Also the filter temperature is correlated with the time at the top of the graph. The graph indicates that neon is trapped in the filter in large quantities. To the far right is the measured intensity of the compressor gas and next to it various measurements of know calibration gases.

neon and hydrogen. However there is very little evidence of having these filters plug and stop operation of the 1400.

It has also been noted that the 1400 charcoal filters that are installed for trapping of nitrogen and oxygen operates at a temperature below the phase transition to solid. In the 800 watt refrigerator the charcoal traps operate slightly above the phase transition to liquid for nitrogen. If the process of trapping nitrogen is dependent upon it forming small solid clumps, then the traps on the 800 watt refrigerator may not be doing their job.

Summary

Although at this time we do not understand the precise contaminate that these micron filter traps are removing, we can state with great assurance that these filters in the liquid helium stream have made a significant improvement in cryogenic system reliability.

K500 VACUUM MEASUREMENTS

M.L. Mallory, E.D. Hudson[a], P.S. Miller, J. Kuchar

The pressure in the K500 superconducting cyclotron was measured as a function of radius for various gas flow rates emanating from the internal PIG source, in order to evaluate the effectiveness of the unique internal cryopumping system. For the test a nude ion gauge with vertical dimensions less than 2.3 cm was built and mounted on the internal beam probe. Figure 1 is a picture of the nude gauge inside the cyclotron. The effect of magnetic field on the ion gauge reading was determined and a method of

Fig. 1 A photograph of the nude ion gauge mounted on the internal probe of the K500 cyclotron.

degaussing the cyclotron devised. Figure 2 is the measurement of pressure versus radius for nitrogen gas of various flow rates. The pressure increases near the outside radius of the cyclotron, possibly reflecting reduced conductanace to the pumps. As the gas flow is increased, the pressure rises faster at the cyclotron center than at larger radii. Data

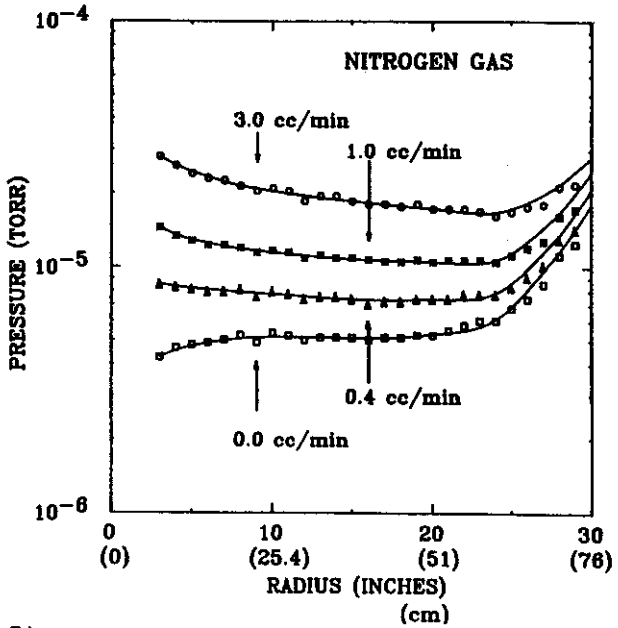

Fig. 2 The pressure versus radius is shown for various nitrogen gas flow rates. The gas was added to the vacuum space through the PIG source gas line.

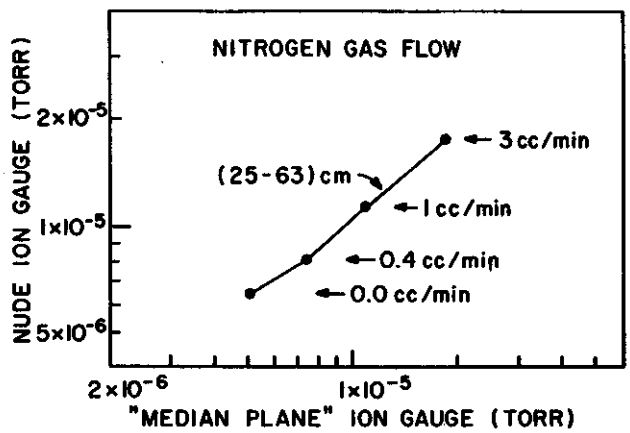

Fig. 3 The nude ion gauge pressure is correlated with the median plane ion gauge in the above graph.

from the normal shielded ion gauge (median plane gauge) located approximately 6m away from the median plane was correlated with the internal vacuum measurements and is shown in Figure 3.

---

a. Oak Ridge National Lab.

A NEW VIEWER PORT PROBE FOR THE K500 CYCLOTRON

B.F. Milton

During commissioning of the K500 cyclotron a relatively simple 2 jaw radial probe was installed in the extraction region. The success of this device led to a decision to construct a more sophisticated model which could be removed under vacuum and would increase the travel from 4" to 12". After extensive design and assembly work in 1985 such a device was installed in the cyclotron in November of that year.

Figure 1 is a schematic view of the probe as constructed. During normal operation the lower table is locked in the inner most position and the upper table (a precision slide table) is moved in or out with a ball screw driven by a stepping motor. In this 'running' condition the moving vacuum seal is provided by the stainless steel bellows mounted between the front plate and the upper table. To remove the probe the lower table is driven to it's outer limit so that the end of the guide tube is in the lock chamber and then the gate valve is closed. During this operation a pair of viton O-rings separated by a floating spacer ring (all labeled sliding O-ring in Fig. 1) provides the vacuum seal. This division of seals means that the bulk of the time (during regular probe travel) the bellows are used but for changing the probe, when the travel is 40" then the O-rings are used. The lower table is mounted on Thomson pillow blocks, and driven by a ball screw attached to a synchronous motor. A complete probe change can be accomplished in half an hour, making repairs and modifications relatively simple.

Another important feature of this design is the ability to accept any probe which meets a few simple requirements; that it matches the bolt pattern on the plate, and that the maximum diameter from the plate inwards is 5/8". The length of the probe from the mounting flange to

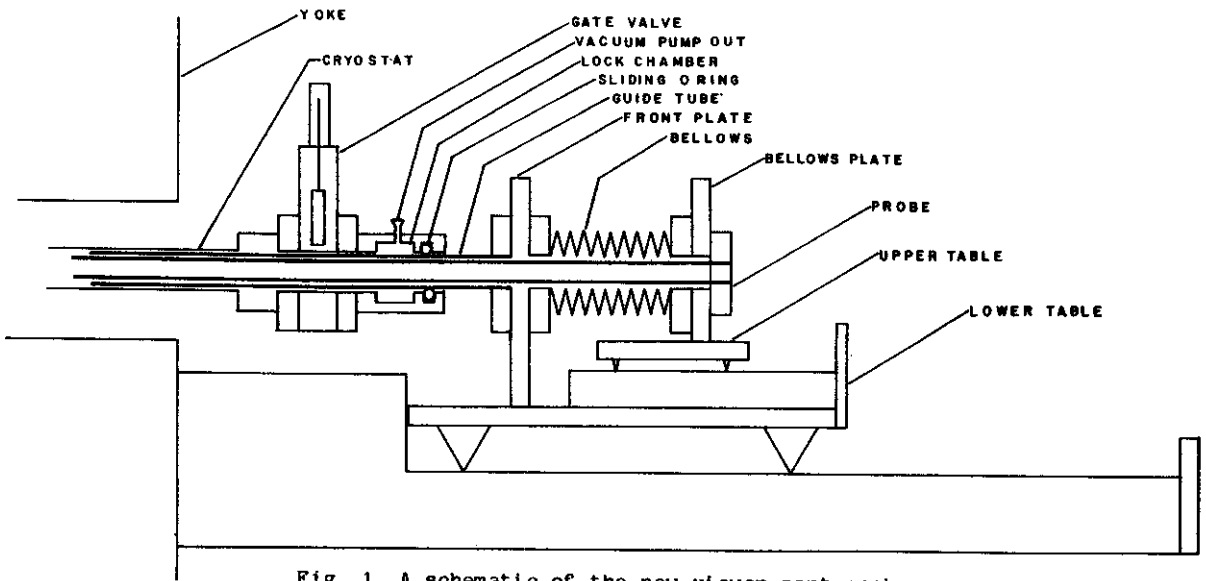

Fig. 1 A schematic of the new viewer port probe drive showing the major components. The two separate drive systems allow for a bellows to be used in the regular range of travel and O-rings to be used for insertion and removal.

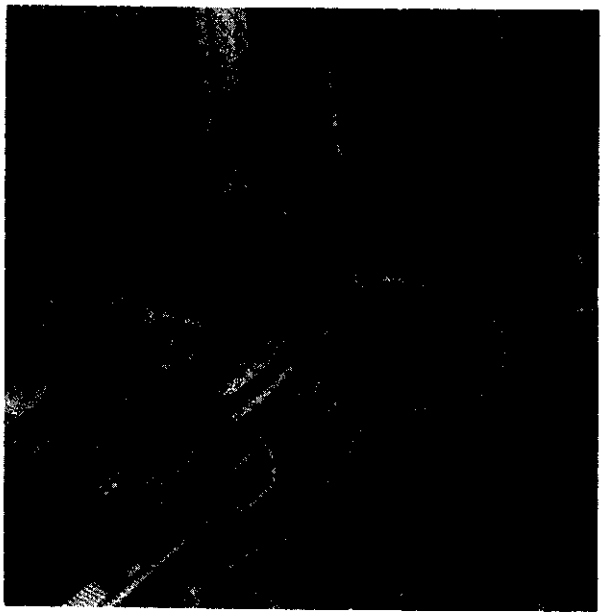

Fig. 2 A photo of the new drive installed on the cyclotron. In this photo the drive is in the 'running' position and a probe is installed.

the tip maybe anything from 45.5" to 59.325". Presently four different probes have been constructed, although not all tested. The first design tested is shown in figure 3. The object of this design was to provide isolated water and electrical circuits within the limited space. It also provided fairly good positioning of the tungsten jaws to ensure the correct differential lengths. Unfortunately the Kovar feed-thrus were poor thermal conductors so when the full beam hit the probe for any length of time the temperature of the jaws rose dramatically and eventually the feed-thrus became electrical conductors. The design currently in regular use is shown in figure 4. This design is the same as that orginally used with the 4" drive but with length changed. Also the jaws are now a single piece of molybdenum which should improve

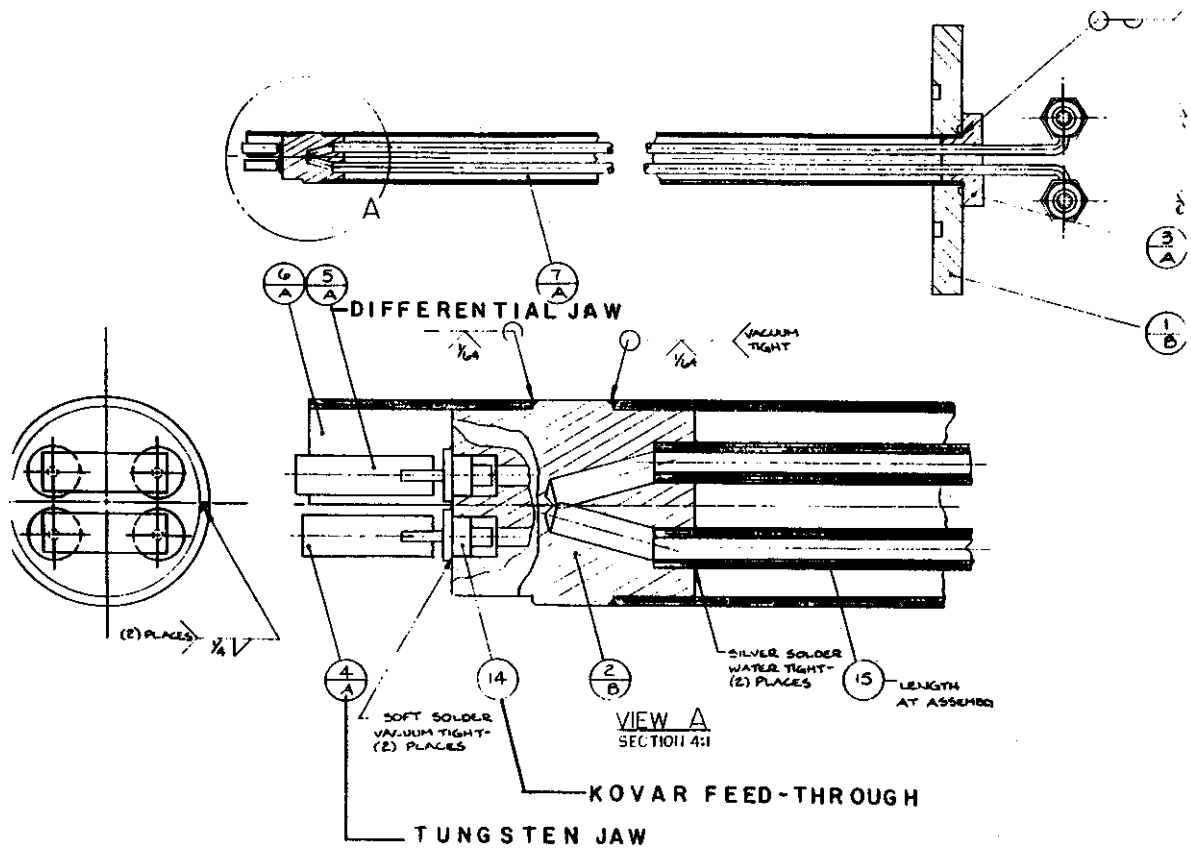

Fig. 3 The first probe used with the new drive. The Kovar insulators were not sufficiently good thermal conductors, resulting in their becoming electrically conducting so this design was discarded.

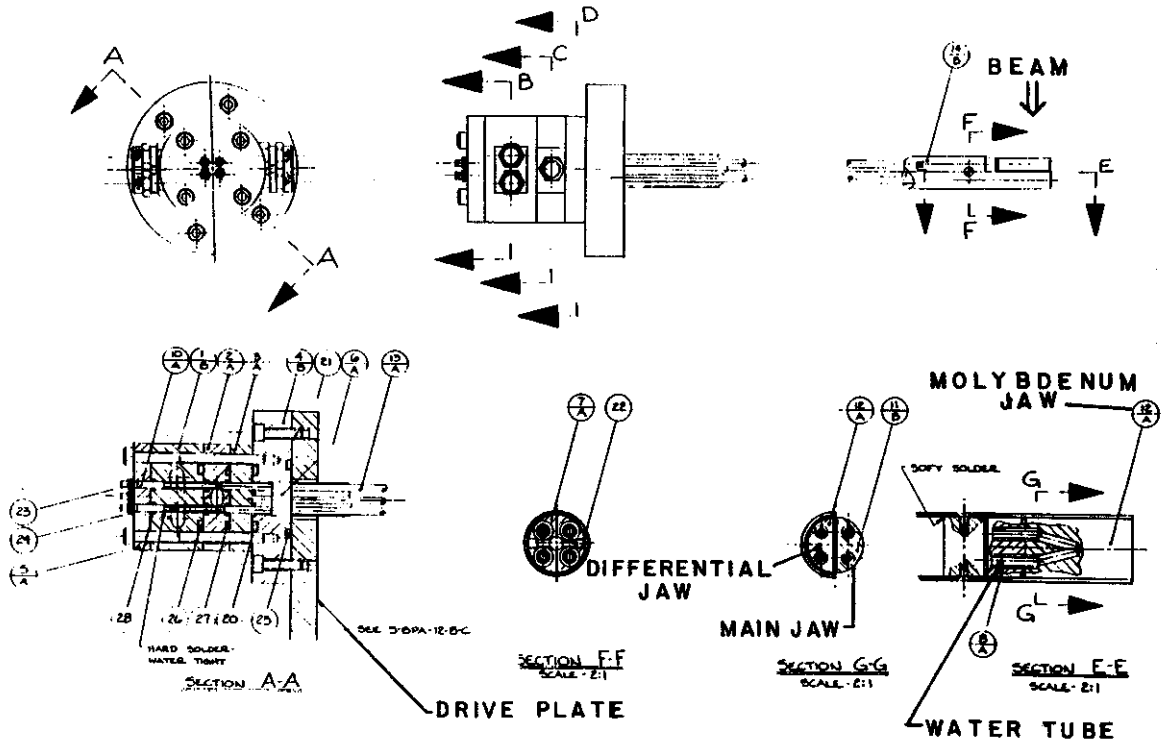

Fig . 4 The 2 jaw differential probe currently in regular use. This design has proved to be very robust.

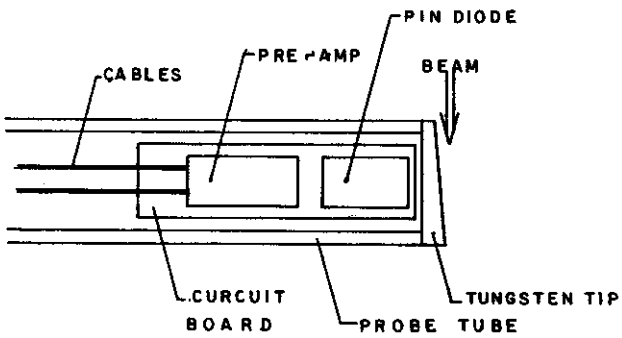

Fig. 5 A schematic drawing of the phase probe. The PIN diode is used to detect gamma rays produced when the beam strikes the probe tip. The small size of the diode and amplifier allows it to be located near the probe tip so the count rates are high and the source is distinct from the background.

the cooling while reducing the possibility of producing alpha emitters. One of the other probes developed is the target for the radioactive beam experiment which is described in another article. The fourth probe, which is still under test, is designed to measure the phase of the beam. This is to be done by detecting the gamma rays which are generated from the beam striking the probe tip with a PIN diode located just behind the probe tip. A schematic of the phase probe is shown in figure 5. The output of the amplifier is used as the start signal for a TAC whose stop signal is the positive zero crossing of the RF. This produces a spectrum of time of the beam hitting the probe vs the RF time which allows the phase width and changes in the phase to be determined.

PHASE SELECTION IN THE K500 CYCLOTRON

B.F. Milton

Phase Selection is usually used in cyclotrons when it is desired to achieve single turn extraction and its associated benefits[1]. Although we eventually wish to take advantage of this, our initial goal is to achieve separated turns over most of the acceleration region so that detailed accelerator studies can be carried out. As shown in figure 1 the high magnetic field in the K500 cyclotron leads to a turn separation which is rather small compared to the turn width associated with the phase spread. If

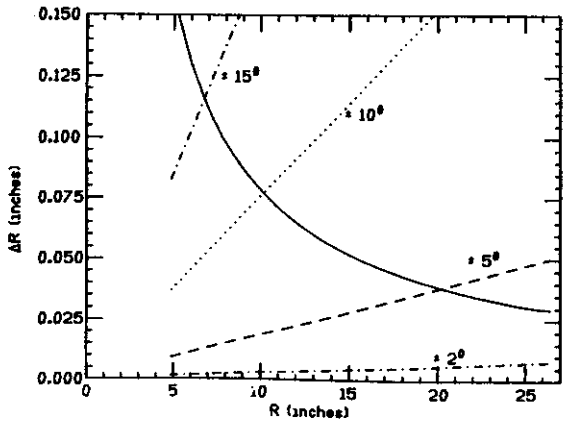

Fig. 1 Plotted are simple estimates of the turn separation and turn widths associated with different phase widths. The turn separation (solid curve) is estimated using $\Delta R=\Delta E*R/2*E$ while the full width of a turn with a given $\Delta\phi$ is found using $\Delta R=(\Delta\phi)^2*R/4$.

one also includes the spatial extent of the beam (the x,p_x size) then it is apparent that with the $\pm 15^0$ phase width transmitted by the central region, that distinct turns would be observable only for the first few inches. If on the other hand the phase width was reduced to $\pm 2^0$, separated turns would be observable for most of the acceleration process and beam centering could be determined. Centering is of great practical importance because it reduces phase oscillations, minimizes the effects of non-linearities and makes extraction insensitive to the dee voltage[2]. Observable turns would also allow the the measurement of the radial focusing frequency ν_r, and with an induced coherent oscillation, the axial frequency ν_z.

Phase selection in cyclotrons is done by taking advantage of the coupling between the radial (r,p_r) and longitudinal $(E-\phi)$ motions of the particles[3]. This technique can also be viewed as using the phase dependant centering of the particles to separate the different phases. Figure 2 gives a typical plot of radius versus starting time. Note the horse shoe shape, with

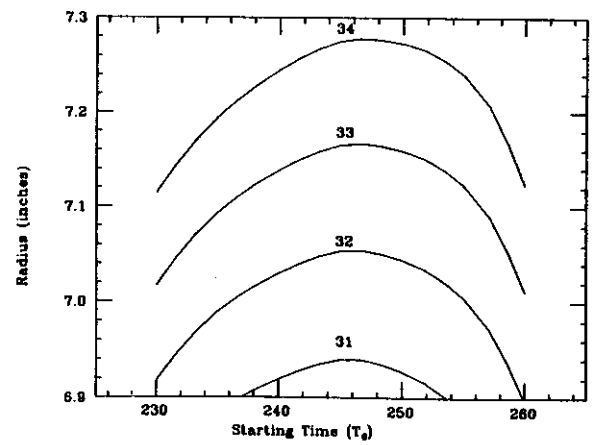

Fig. 2 The radius of the central ray is shown as a function of starting time for four successive turns. Note the typical horse-shoe shape resulting from the $\cos(\phi)$ dependence of the energy gain.

the peak occurring at the starting time which has had the largest average energy gain per turn up to that point. This plot immediately demonstrates how a physical obstruction which blocks some radii would select particles with particular phases. It also is a good example of why too large a phase spread will produce fractured groups of "allowed" starting times as opposed to the single group desired, because

with a large phase spread there is more than one starting time at the same radius. The solution to this situation is to perform the selection process in two stages.

The first stage is a coarse selection located near the center of the machine where the large turn separation allows the installation of a slit with a large enough frame to avoid the possibility of undesired phases passing around the frame. If such a system were designed to transmit only 20^0 of phase the situation illustrated in figure 2 would be single valued. In Fig. 3 such an aperture is shown for the first harmonic central region using a Penning Ion source. In this figure we have superimposed

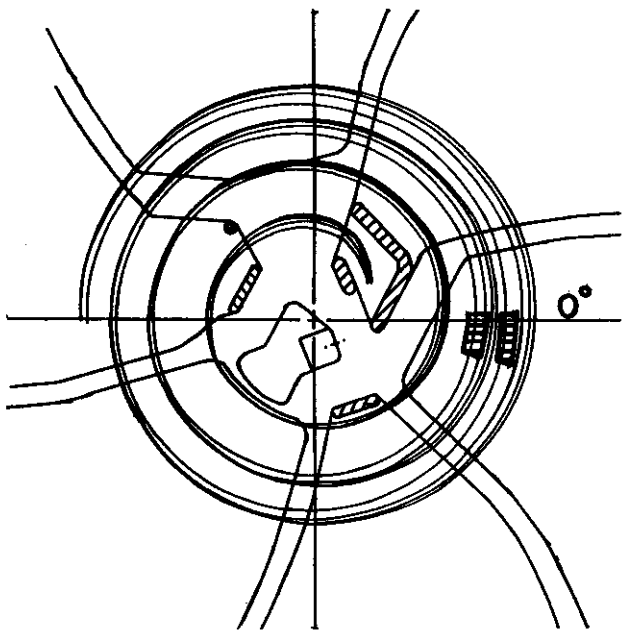

Fig. 3 Electrode structure for the K500 first harmonic central region using a PIG source. Four orbits are shown corresponding to starting times τ_0=230,240,250, and 260 degrees. The peak electric field between the source and puller is achieved at τ_0=270. A slit is located on the 0° hill extension of the center plug allowing easy installation and removal. This slit removes all starting times which do not fall between 230 and 250 degrees.

4 orbits on a median plane section of the central region electrode structure. The four rays have starting times ,τ_0 ,of 230^0,240^0,250^0, and 260^0 and an initial $x=p_x=0$. As shown only the 240^0 and 250^0 rays pass through the slot formed by a U shaped block mounted on the hill portion of the center plug, (230^0 almost does). By locating the slit on the center plug it could be removed and inserted by pulling the center plug, a considerably easier task than raising the magnet cap. Since a τ_0 of 270^0 corresponds to the peak electric field in the source to puller gap it is unlikely that many ions outside the 230^0-260^0 range shown can enter the first turn. In the case of later starting times (towards 270^0) there is insufficient time to cross the source to puller gap, and for the earlier times there is insufficient electric field to pull the ions from the source. The solution in the case of an axially injected beam is quite different as shown in figure 4 for a first harmonic mode. In this central region the

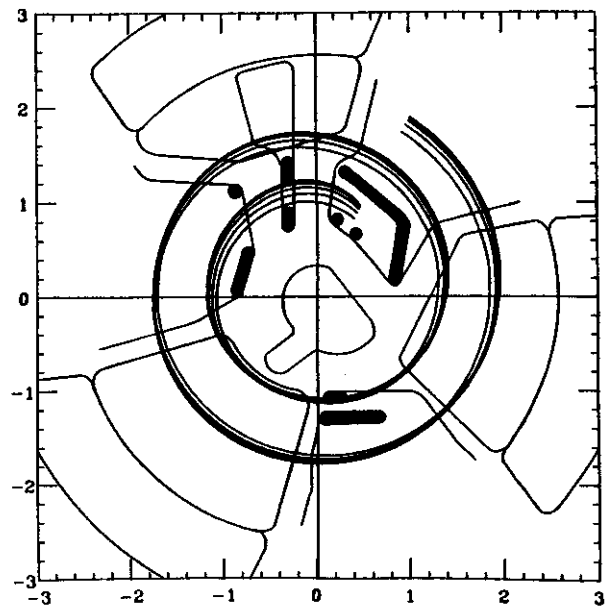

Fig. 4 The electrode structure for the first harmonic central region with axial injection. Five orbits are shown corresponding to starting times of 230,240,250,260, and 270(inner most in radius) degrees. The window frame attached to the dummy dee following the puller is used to neutralize the coupling between the first and second dees. By narrowing the radial width of this window it will be easy to remove those starting times lying outside 245° to 260°.

RF coupling between dees is neutralized by a window frame structure mounted on the dummy dee which screens one dee from another. By enlarging the radial extent of the vertical sections of this frame it can also be used to select a group of starting times, in this case between 245° and 260°. With this particular central region the τ_0=250° ray has the least centering error at 15", whereas in the PIG case best centering occurred for the ray with τ_0=240°. In both cases the allowed phase spread is approximately ± 10° around the "centered" orbit.

It seems natural to wonder why a phase selection system is necessary when the beam is being axially injected, since the beam can be pre-bunched before entering the cyclotron. In fact we do plan to use a buncher located just before the entry into the cyclotron yoke but there is a fair amount of de-bunching of the beam as it traverses the yoke[4] and inflector. This debunching is illustrated in Fig. 5 where the difference in starting times is plotted as a function of particle number (there are 8 particles distributed around the perimeter of an ellipse). As the bunched beam will have a phase spread in the neighborhood of ten degrees the beam entering the cyclotron will again have a phase spread of thirty degrees, the only difference now is that the buncher phase is an extra adjustable parameter. In the case of the axially injected beam there is a further concern that the non-linearities in the spiral inflector will produce a distorted phase space which could make phase selection difficult. To reduce this effect we will work with a small beam spot for the accelerator studies. It was found that if the analysis system in the beam transport system was used to select a beam with an emittance of 25π mm-mrad (unnormalized) then after the strong focusing that takes place during the yoke traversal the beam spot size at the entrance to the inflector would be 1 mm in diameter. The gap in the inflector is 4 mm so a 1 mm beam

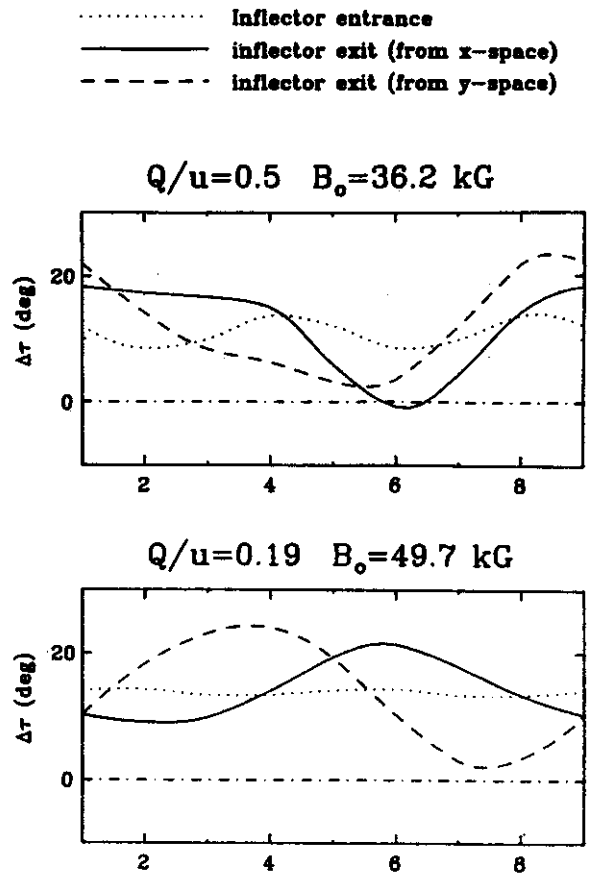

Fig. 5 RF time differences for the particles on the boundary of a 100π mm-mrad phase space with respect to the central ray. The dotted line indicates the difference at the entrance of the inflector. The solid and dashed lines show the differences at the inflector exit. The abscissa is just an arbitrary parameter around the boundary of the phase space.

should pass through sufficiently far away from the electrodes to avoid serious non-linearities as shown in the x-p_x plot of Fig. 6 at the exit of the inflector. To insure that the spot size at the entrance of the inflector is indeed 1 mm in diameter it would be simple to replace the collimator at the inflector entrance with one with a 1 mm hole instead of the usual 4 mm. It is expected that the beam intensity change associated with the emittance change from the usual axial injection value of 100π m-mrad to the 25π mm-mrad we desire will not significantly limit accelerator studies since we plan to use a low charge state beam such as $^{16}O^{4+}$ which can be

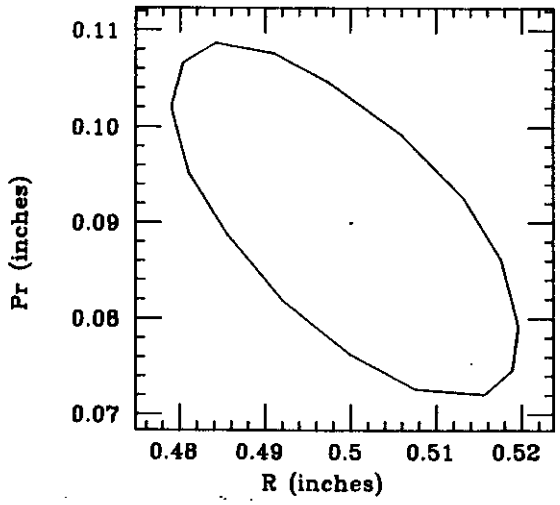

Fig. 6 The phase space at the exit of the inflector when the initial beam has an emittance of 25π mm-mrad. The momenta have been divided by qB_0 to express them in units of length.

produced by the ECR source in copious amounts. As far as distortions are concerned the only remaining question is whether or not the electric fields on the first few turns would distort the phase space. In Fig. 7 we show the results when a group of eight rays populating the perimeter of the ellipse shown in Fig. 6 are accelerated forward 3 turns using the program "CYCLONE" which integrates the equations of motion in the measured magnetic field and in an electric field computed with a relaxation code. For each ray several different starting times were run so the values of R and P_r at the the final position are plotted as a function of the average phase on the last turn. By interpolating to get the R,P_r values for the particles with the same average phase we get the ellipse shown in Fig. 7, which is almost distortion free, as desired. The use of particles with the same average phase is particularly important since these are the particles which will have the same energy gain per turn so they will all arrive at the deflector with the same energy. Also by using this grouping of the particles one avoids an apparent distortion which is actually due to the energy dependence of R and P_r.

At this point we have a well behaved beam which has exited the central region with a phase width of approximately 20° and it remains to reduce this to something in the territory of 4° or 5°. As is apparent in figure 1 at this level of phase selection the radius spread due to the

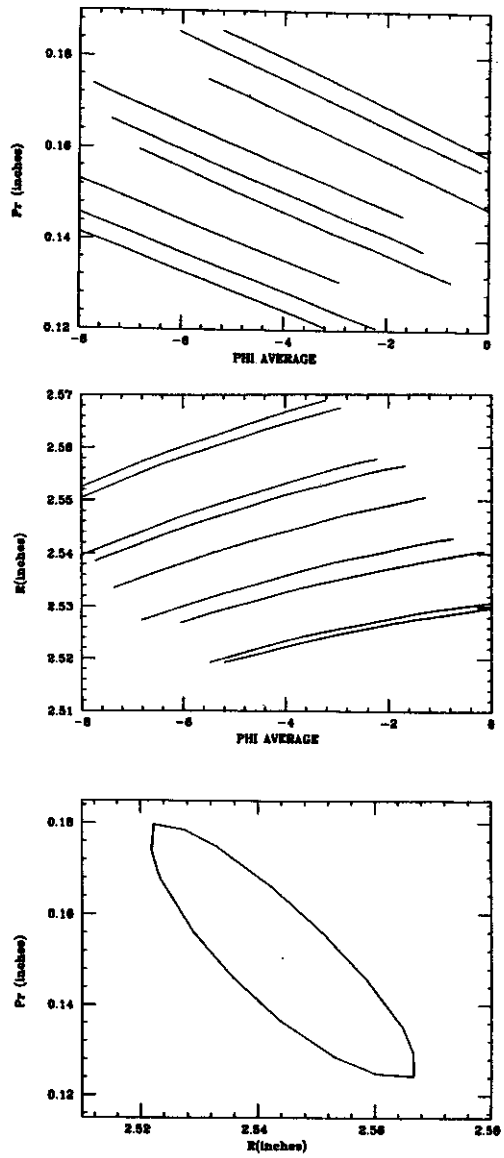

Fig. 7 The R and Pr are plotted for a group of rays which started on the perimeter of the ellipse shown in Fig. 6, after 3 turns, as functions of the their average phase. In the third frame the results of interpolating to find each ray at an average phase of -4° is shown. Note the ellipse shows no distortion.

phase is comparable to the beam spot size, so the interaction between these two must be taken into account. To achieve the best possible selection one would like to place the next set of obstructions where Q, defined by[5]:

$$Q=(\Delta R)/(\Delta\phi)$$

is a maximum. At the same time it is advantageous to do the selection as near as possible to the center of the machine where the beam energy is low, so as to reduce the possible activation of the cyclotron components which is one of the goals of such a system. In figure 8 we plot the radius differences r_i-r_0 at a fixed azimuth, where r_0 is the ray which leaves a Penning Ion Source at $\tau_0=235^\circ$ (the results for an axially injected beam are qualitatively the same). At the radius of turn 33 (approximately

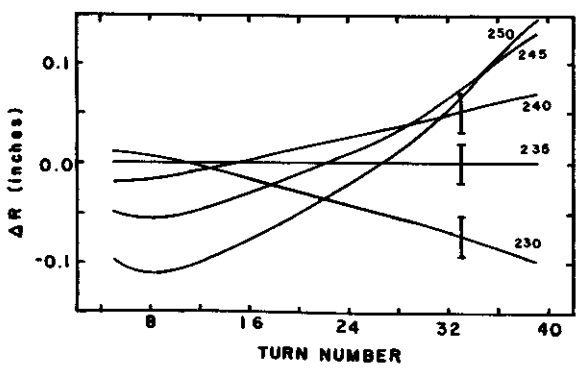

Fig. 8 Radius difference r_i-r_0 at $\theta=84^\circ$ vs turn number for a family of central rays. Ray 0 leaves the source at $\tau_0=235^\circ$, the others at the times labeled on the plot. At turn 33 a bar of ±.02 inches is shown to give an idea of the radius variation expected from the r,pr distribution around the central ray.

7") there is a space between trim coil number 2 and trim coil 3 so at this radius in the center of the hill a 1/2" diameter access hole passes from the liner through the pole and exits on the magnet cap. To preserve the magnetic symmetry there are six such holes but because of the space requirements of the system only two of them are usable, one on hill A and the other on hill B. As can be seen in figure 8 the Q at this radius is quite good while the turn separation is still about 100 mils (see Fig. 1) and the energy is only 6% of the extraction energy. Included in this figure is a bar of ± .02 inches, which is intended to give an indication of the radius variation expected from the x,p_x distribution around the "central ray".

A more detailed analysis involving the x,p_x spread of the beam is presented in figure 9. In this figure we have plotted the radius against a pseudo starting time, for three successive turns at the location of the phase slit holes. The horizontal label is referred to as a pseudo starting time as the actual starting times for rays with different values of r,p_r have been adjusted[6] so all rays with the same horizontal label will have the same energy gain per turn. In the first and fourth (numbering from left to right) the situation is shown with both slit mechanisms[7] retracted. In the second and fifth frames the results are shown after a 60 mil blade has been inserted at an azimuth of 84° (upper slit mechanism). It can be seen that this blade provides most of the phase selection desired but it is still necessary to eliminate those unwanted particles whose betatron oscillations have placed them at the same radius as particles with a desired phase. To do this final cleaning up operation a second slit is required. At this radius in the K500 the radial focusing frequency ν_r is close to 1.0 so after the azimuth has changed by 120 $^\circ$ those particles which had large x components, that moved them towards the radius of the desired phases, will now have a radius which is away from the desired phases as illustrated in figure 10. In the third and sixth frames of Fig. 9 the result of placing such an obstruction at an azimuth of 204° (lower slit mechanism) is shown. The group of rays present in the final turn have a phase spread of $\pm2^\circ$ around the chosen central phase. By correctly tailoring the phase curve and the RF frequency the particles with the central

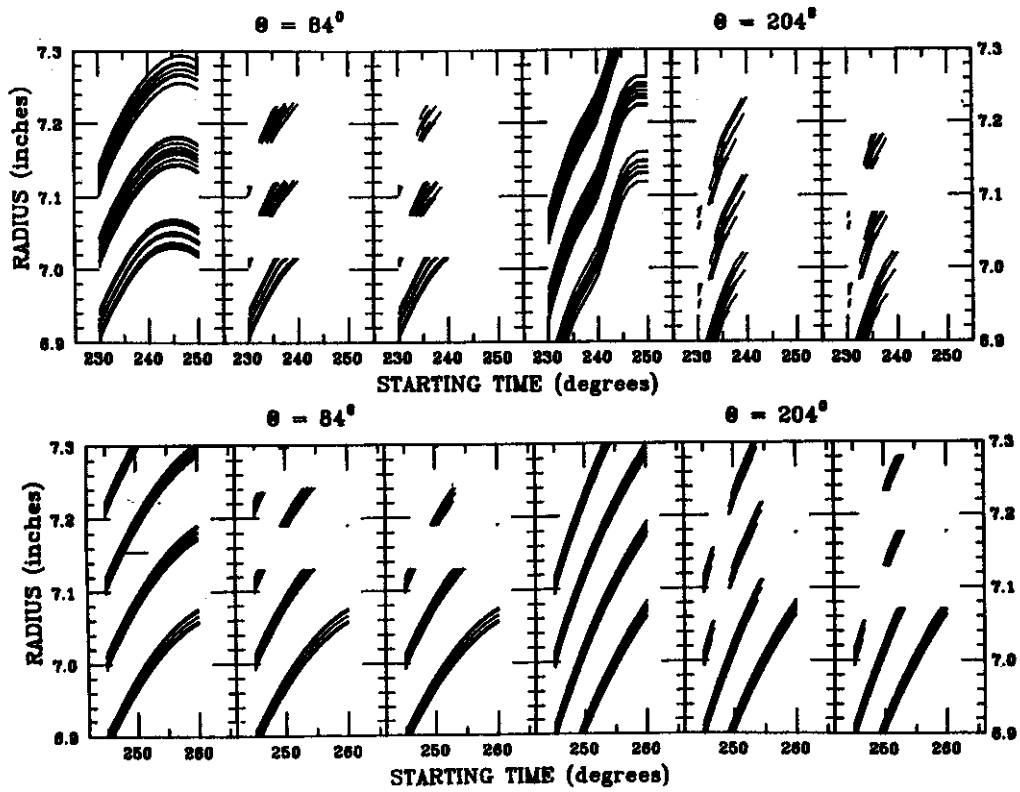

Fig. 9 Radius is plotted as a function of the starting time for turns 32,33 and 33 for the PIG geometry in the upper sequence and for turns 29 through 32 in the lower plot for the ECR geometry. Associated with each central ray is a set of 8 rays which populate the circumference of a .02 inch radius circle in R,Pr space. From left to right: the first one shows the situation at θ=84 before the blades are inserted, the next one shows the situation after a 60 mil blade has been inserted at 84° and the third shows the effect of inserting a second blade at θ=204°. The following three frames are the same except at θ=204°. Note the final phase width is around 4 degrees and the full .02 inch phase space around the central time survives. The rays with different R,Pr values have a starting phase which gives them the same energy gain per turn as the central ray they are associated with thus the horizontal label is actually a measure of the energy gain per turn.

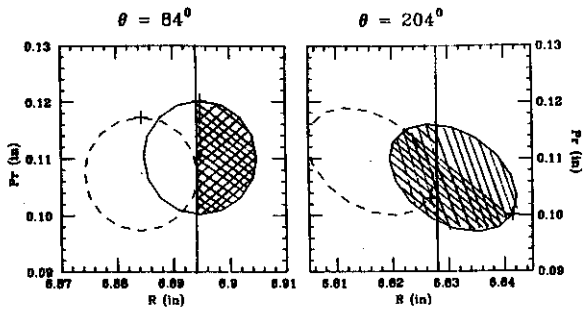

Fig. 10 A simple demonstration of why two slits are required to do a careful phase selection. Shown are two bundles of rays which have a one degree difference in phase. Note that at thefirst azimuth it is impossible to remove all of one phase without effecting the other phase. After the particles have traveled 120° in azimuth they have executed a third of a betatron oscillation as highlighted by the cross which marks the same ray in both frames. As the shading demonstrates it is now possible to remove almost of the unwanted phase.

phase will have the maximum energy (within a given turn) at the outer radii of the machine.

At this point we should explain how a tungsten post (blade) can be used to perform the same function as a slit. The most important feature of this technique is to set the post size such that it affects both the turn on its inside and the one on the outside as modeled in Fig. 11. In this mode the high radius particles are scraped from turn "n" on the inner edge of the blade and the low radius particles from the turn "n+1" on the outer edge of the blade. With $\nu_r \approx 1.0$ the composition of the beam at turn "n+1" is little changed from that at "n" and the post has scraped the high and low radii from the successive turns just as slit would from a single turn.

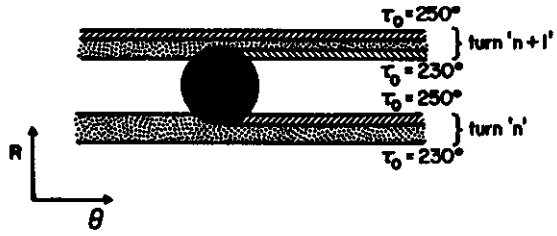

Fig. 11 A schematic of how a single post can act in a manner similar to a slit. The inner edge of the post scraps off those particles with too large a radius, while the outside scrapes off those with too low a radius on the next turn. The dotted region is the surviving beam while the cross hatched region is the removed beam.

As described in another article the drive mechanisms for the phase selection system have been installed; testing with beam is scheduled to begin in the near future.

References

1. M.M. Gordon, IEEE Trans. NS-13(4),48 (1966).
2. J.C. Collins, "Phase Selection Mechanisms in Isochronous Cyclotrons Producing High Resolution Beams", Ph.D. thesis, Michigan State University, 1973, pg. 12.
3. Ibid. pg. 3
4. F. Marti, IEEE Trans. NS-32(5),2450(1985).
5. Cit. loc. 2, pg. 43.
6. M.M. Gordon, Part. Accel. 12,13(1982).
7. B.F. Milton, Construction of Phase Slits For the K500 Cyclotron, this report.

CONSTRUCTION OF THE K500 PHASE SLITS

B.F. Milton, J.A. Kuchar and S.A. Hickson

The plan for phase selection in the K500 cyclotron[1] calls for two small tungsten blades to be inserted between turns 32 and 33 on successive hills. Desirable features of a phase selection system were seen to be easy insertion and removal of the blade from the beam chamber and adjustablity of the slit position (to accomodate different orbit patterns). Also since the lifetime of the blades was uncertain, a large effort was directed at being able to change blades with minimum disruption of cyclotron operation. This last feature also would allow for adjustment of blade size (by changing the blades) which is analogous to changing the slit size in a conventional system. Access to the median plane on the hills consists of two, half inch diameter holes located near the center of hills "A" and "B" at a radius of 7.038". The hole on hill A (θ=83.5^0) exits on the upper pole cap, while the other (θ=203.5^0) exits on the lower cap. This requirement is imposed by the relative locations of the center plug gate valves.

These features are realized by mounting a one inch long tungsten blade (pin) off-center in a small copper cap that is bolted onto the end of a forty inch long stainless steel shaft traversing the magnet poles. Since the pin is located off-axis, rotating the shaft in the access hole results in the desired adjustability in the pins radius (and an unimportant change in it's angle). Moving the shaft up and down by one inch will move the blade in and out of the beam chamber, while pulling the shaft all the way out will allow changing the blades. In actuality the shaft is two concentric stainless steel tubes set up in a spray tube configuration (as shown in Fig. 1) so that the beam end of the shaft is water cooled. This feature indirectly cools the tungsten blade which will intercept the unwanted beam.

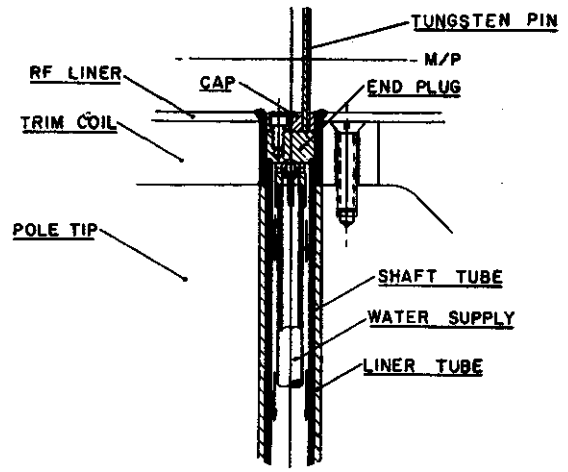

Fig. 1 The end of the shaft at the median plane of the cyclotron. The sixty-two mil tungsten pin intercepts the unwanted beam. The pin is mounted in a copper cap which is easily removed for rapid pin change. Note; the copper end plug is water cooled so the tungsten will be indirectly cooled.

Control of these functions is provided by a mechanism located between the center plug and the dee stem on the pole cap at the exit of the access hole. The access hole lies beneath the flared portion of the dee stem spinning; the limited space available requires the compact and intricate device shown in figure 2. It can be seen in this figure that the mechanism consists of two major groups of parts, those below the bellows which are rigidly fixed to the pole cap, and those above which are moved up and down on a pair of rails by the pneumatic cylinder. It is this one inch of bellows motion which allows the shaft to move so the blade can be inserted into or retracted from the beam chamber.

Located at the top of the moving section is the rotating water manifold. Inlet water

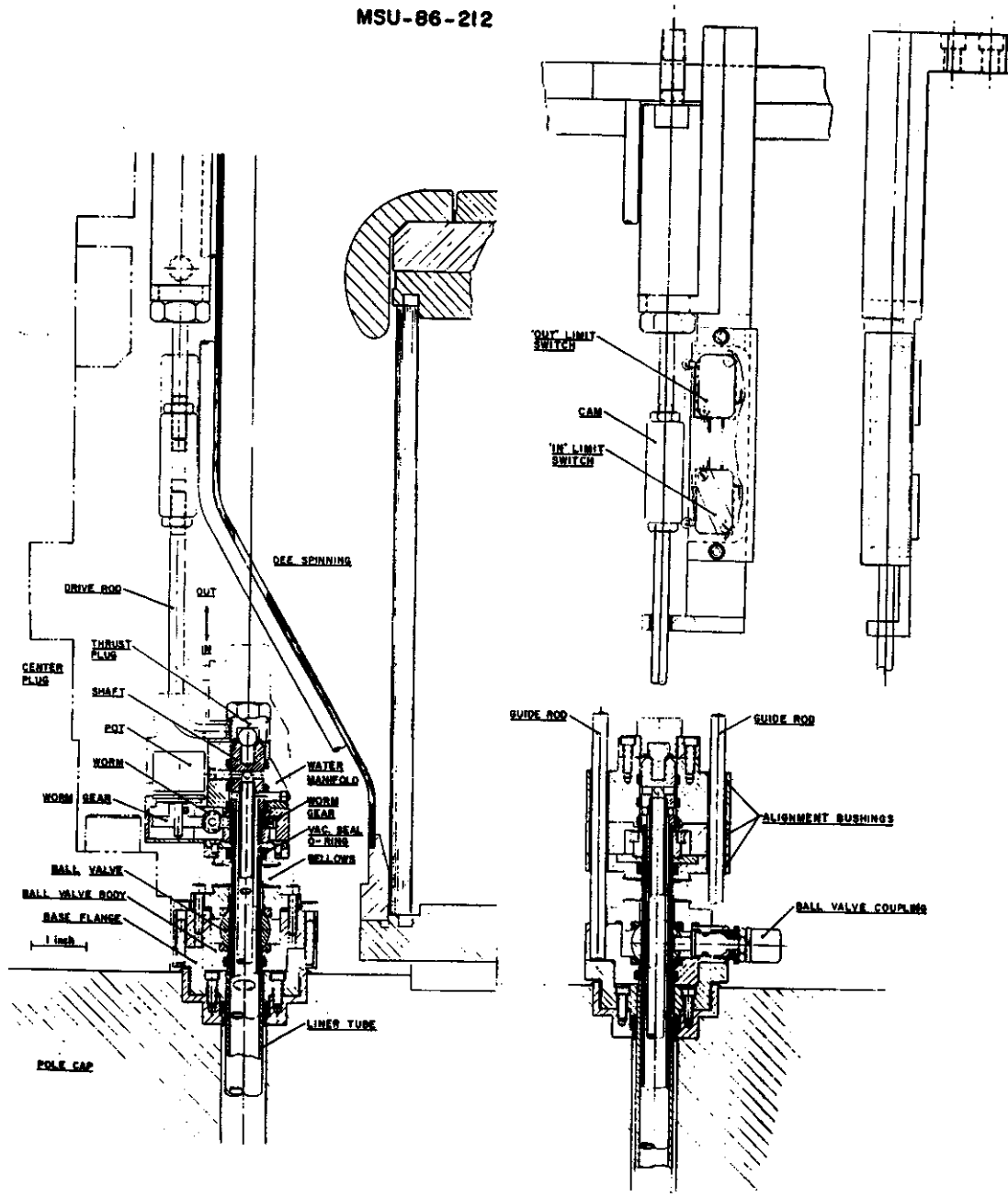

Fig. 2 Cross section of the phase slit drive mechanism. See text for a description.

surrounds the shaft in the small chamber formed by the first two coaxial O-rings, passing through the four radial holes in the shaft to reach the center tube. The water returns from the tip between the inner and outer tubes, exiting through the another set of 4 radial holes into the the small chamber formed by the second and third O-rings. Just below the third O-ring the shaft diameter is reduced to form a shoulder which rests on the worm gear. When the thrust plug screw is tightened this shoulder and the ball bearing in the thrust plug trap the shaft axially so the shaft must travel in and out with the action of the air cylinder. A key on the shaft just below the shoulder mates with a keyway in the worm gear; turning the worm gear causes the shaft to rotate. On the opposite side of the worm, a second worm gear is mounted on a servo potentiometer, providing information about the rotational position of the shaft. The driving worm is driven by a motor mounted three feet away on the dee stem support beam. Torque is transmitted from motor to worm gear by flexible drive cable. This system was chosen so that there would be sufficient room to shield the synchronous motor from the the high magnetic field.

The ability to change the blades with the minimum disruption of cyclotron operation requires removing the shaft without raising the cap or otherwise breaking high vacuum. The blade changing operation begins by removing the thrust plug, exposing a set of threads in the top of the shaft. Removing the two copper patches in the dee stem spinning allows a rod to be passed through the spinning and threaded into the the top of the shaft. Pulling on this rod draws the shaft out of the cyclotron, while the sliding seal O-ring maintains the vacuum. When the piston is in the retracted position the bellows forms a lock chamber sufficient to accomodate the pin and cap assembly. The ball valve can then be closed using a 1/4" drive rachet wrench to turn the the brass ball valve coupling one quarter turn. Once the valve is closed the shaft can be retracted the rest of the way. Insertion is accomplished by reversing these operations.

The parts below the ball valve form the mount for the rest of the assembly. The base flange is threaded so that it screws onto the tube which separates the liner vacuum from the main vacuum. When fully threaded on it also compresses the O-ring making the liner vacuum seal. To prevent this flange from backing off screws pass through 4 of the 12 clearance holes in it and thread into the pole cap. The redundant clearance holes were necessary since the point at which the threads on the linear tube would bottom out was unknown. Above the base flange is the ball valve body, which is also the support for the guide rails. Since the guide rails must have the correct orientation relative to the dee stem, all orientations were made possible by having the bolts holding the ball valve body to the base plate pass through thirty-degree-wide clearance slots to pick-up four of the twelve available threaded holes in the base plate.

The photograph in figure 3 show the upper

Fig. 3 The lower phase slit hole before the trim coil leads were moved.

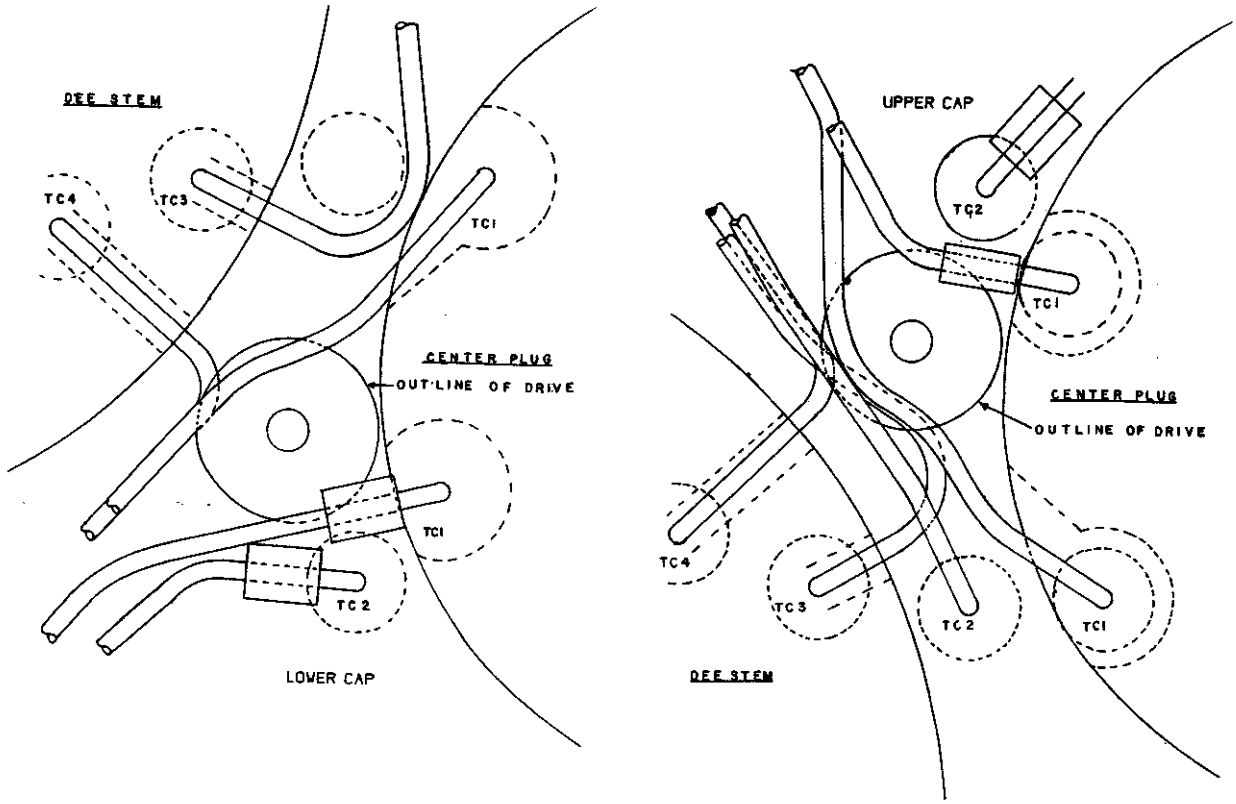

Fig. 4 A schematic of the trim coil leads in their positions before moving. It can been seen that in both cases several leads encroached on the phase slit drive space quite seriously.

and lower phase slits holes before installation. As can be seen in this figure and in Fig. 4, some trim coil leads pass through the space required by the phase slit drive. This would not be true had the leads conformed to the designed configuration therefore the first part of the installation process was devoted to re-routing the errant leads. To facilitate this operation both the upper and lower center plugs were removed. Next the center plug extensions and the gate valves were removed. After removal of the the hill extensions, the center plug liners were unbolted and pulled out as far as the dee spinnings would allow, about six inches. This disassembly exposed the flare fittings on trim coil #1, and improved the access to the fittings on some of the other trim coils. In all cases the leads were either cut or unsoldered at the transitions between the 1/4" and 3/8" copper tube. In those cases where the feed-throughs were exposed, the flare fittings were undone and the segment of 1/4" line was re-manufactured. For trim coils #3 and #4 on the upper cap and trim coil #4 on the lower cap, the feed-through lies beneath the dee stem spinning. Here, with the cut end free, the leads were bent using the modified pliers shown in figure 5. During this operation care was taken to apply as little force to the feed-throughs as possible, as they are known to be fragile. With a little practice this bending technique proved to be quite efficient and simple. After the bending was complete the leads were re-insulated, the transitions were soldered together, and the leads water tested. At this point we also cleaned all the feed-throughs and repaired any

Fig. 5 The special pliers built to allow bending those leads which were trapped under the dee stem spinning. With a little care they could be used to move the leads without crimping the lead or putting force on the feed-through.

damaged insulation on any of the other coils. (This work seems to have removed a short which existed in lower trim coil #1.)

With the trim coil leads in the proper locations, the phase slit base plate could be screwed on and the center plug liner re-installed, thus restoring the liner vacuum. Next came the task of making the access holes in the dee stem spinning and spinning flanges. Location of these holes was accomplished using the special tooling fixture shown in Fig. 6. The rod with the sharpened point was passed through the pole to the median plane, so striking the rod with a hammer created a locating mark on the spinning. Using a right angle drill and a 19/32" bit, a hole was drilled perpendicular to the surface of the spinning and centered on the punch mark. With a hand file, the hole was enlarged in the vertical direction so that an oval shaped hole was formed which would allow a 9/16" shaft to pass through freely. The holes in the upper flange were drilled using a portable drill press, while the lower ones were done with a hand drill motor. In both cases the drill was guided by the drill

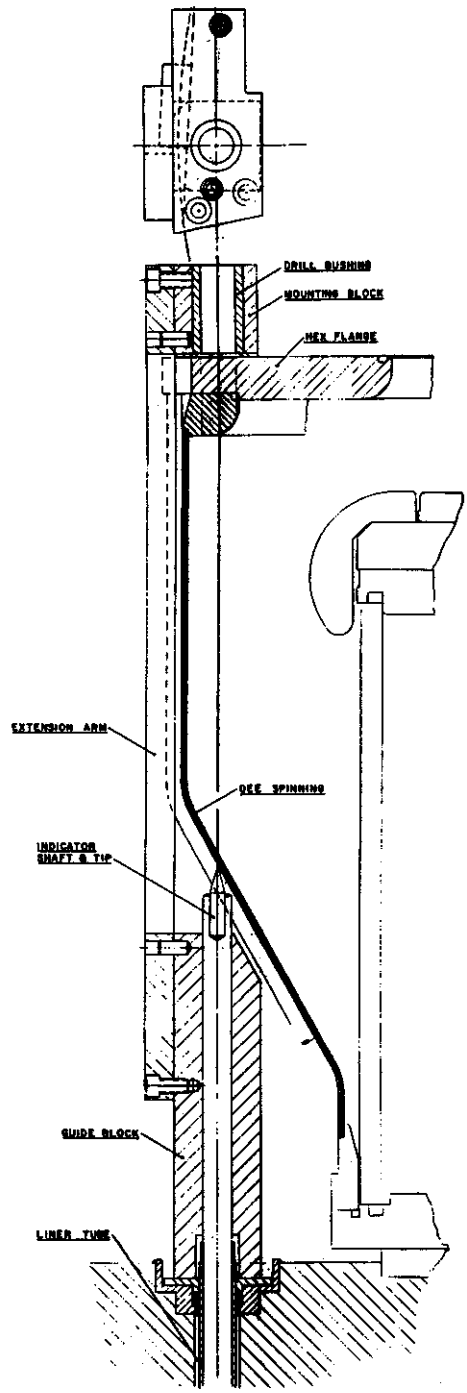

Fig. 6 The fixture used for locating the hole in the dee stem spinning. The other end of the indicator shaft was at the median plane so it could be tapped with a hammer to mark spinning with the sharpened point. The drill bushings provided alignment of the clearance hole and the two threaded holes for mounting the air cylinder on the hex flange.

bushings in the locating fixture.

In order for the half-inch shaft to freely pass through to the median plane, the bead formed where the liner tube is welded to the liner was cleaned up with a combination of oversized hand reamers and a file. With this work complete, the drive mechanisms could be mounted and the shafts installed.

After the motors were installed it was found that there was excessive wind-up in the flexible drive cables. This difficulty was resolved by changing to a larger diameter drive cable and improving the alignment of the worm gear and the worm. With these modifications the drive was found to perform quite well.

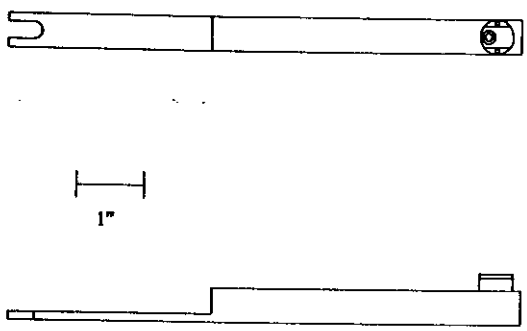

Fig. 7 The fixture used for setting the angle of the drive. The cap on the end fits over the end of the shaft when the normal cap with pin is removed. The notch fits over the post on the center locating fixture so the rotation of the shaft is determined at either 0° or 180°.

To calibrate the position of the pin the fixture shown in Fig. 7 is used. By placing the U shaped slot over the dowel pin in the dee locating fixture and rotating the phase slit shaft until the cap fits onto the the end of the shaft, the location of zero degrees can be found.

The complete installation of the phase slits excluding the drive cable modification and alignment took close to two weeks to complete. Over half of that time was devoted to re-routing the trim coil leads.

References

1. Phase Selection in the K500 cyclotron, B F. Milton, this report.